THE INVESTIGATION OF SENSORLESS CONTROL METHODS OF INDUCTION MACHINES FOR LOW SPEED OPERATION

A DISSERTATION

Submitted in partial fulfilment of the

requirements for the award of the degree

of

MASTER OF TECHNOLOGY

in

ELECTRICAL ENGINEERING

(With specialization in Electric Drives and Power Electronics)

By

MEDA REVATHI

DEPARTMENT OF ELECTRICAL ENGINEERING
INDIAN INSTITUTE OF TECHNOLOGY ROORKEE
ROORKEE - 247 667 (INDIA)
MAY, 2016

INDIAN INSTITUTE OF TECHNOLOGY ROORKEE
CANDIDATE'S DECLARATION

I hereby certify that the work presented in the dissertation report entitled **"The investigation of Sensorless control methods of Induction machines for low speed operation"**, as a part of curriculum for award of the degree of "**Master of Technology in Electrical Engineering**" with specialization in Electric Drives & Power Electronics and submitted in the Department of Electrical Engineering of Indian Institute of Technology Roorkee, Roorkee, is an authentic record of my own work carried out during the period June 2015 through May 2016, under the supervision of **Dr. M.K. PATHAK**, Associate Professor, Department of Electrical Engineering, Indian Institute of Technology Roorkee and **Dr. PETER LANDSMANN**, Chair: **Prof. RALPH KENNEL**, Department of Electrical and Computer Engineering, Technical University of Munich, Germany.

Date: May 23rd, 2016

Place: Roorkee   **REVATHI MEDA**

CERTIFICATE

This is to certify that the above statement made by the candidate is correct to the best of my knowledge.

Dr. M. K. PATHAK

Associate Professor,

Dept. of Electrical Engineering,

IIT Roorkee,

Roorkee -247 667 (India)

ACKNOWLEDGEMENTS

ABSTRACT

This dissertation report describes the investigation of sensor less control methods of Induction machines for low speed operation.

Requirement of low cost, low maintenance, robust electrical motors has resulted in the emergence of the AC Induction motor as the industry leader. Induction motors have been used more in the industrial variable speed drive system with the development of vector control technology. This method requires a speed sensor such as shaft encoder for speed control. Sensors used in electric drives degrade the reliability of the system especially in hostile environments and require special attention to electrical noise. Moreover, it is difficult to mount sensors in certain applications in addition to extra expenses involved. The induction motor drives without mechanical speed sensors have low cost and size and high reliability.

IM is mathematically modelled to get an approximate idea of the actual plant model. The vector control of IM is implemented by using PI controller. To make the system sensor less, we go for rotor speed estimation using MRAS technique along with Popov's hyper stability criteria. MRAS identification is performed with three methods based on rotor flux, back emf and reactive power as the state variables. The different simulation results are observed and studied and the analysis of the different simulated results are presented.

The dynamic performance of the estimators is analysed for parameter variations with particular focus on low speed operation. The Reactive power based MRAS method is observed to be the best method and tested with experimental setup on 400V test bench.

CONTENTS

LIST OF FIGURES

1. INTRODUCTION

1.1 General

With development in power electronics, variable speed applications of both AC and DC machines gained momentum. DC drives use thyristor controlled rectifiers to provide high performance speed, torque and flux control. Traditionally most of the industrial applications that require better torque, speed or position control use the DC motors. But, the advantages of induction motors are clear in terms of reliability, robustness, high torque to weight ratio, price and ability to operate in hazardous environment. After the development and implementation of vector control of induction motors, they are able to compete with DC motors in high performance applications. The dynamics of Induction machine is comparable to that of a DC machine with fast transient response if the torque producing component and the flux producing component of stator current are controllable independently which means it is possible to control the magnitude and phase angle independently.

Over the past few years, the interest in sensor less control of induction motor (IM) has grown significantly due to the advantages such as simple construction, mechanical robustness and less maintenance. The applications include fans and pumps, subway and locomotive propulsions, paper and textile mills, machine tools and robotics, electric and hybrid vehicles, heat pumps and air conditioners, wind generation systems, rolling mills, home appliances etc. So, with the development of vector control technology, Induction machines have been used more in the industrial variable speed applications. But this method requires a speed sensor such as shaft encoder for speed control.

On the other hand, a shaft encoder can't be mounted in some cases such as high speed drives and motor drives in a hostile environment. Moreover, it involves careful cabling arrangements with attention to electrical noise. In addition, it becomes bulky in the motor size and expensive in the system price. Therefore, it has some demerits in both mechanical and economical aspects. Thus the current research efforts are focused on "sensor less" vector control problem, to increase reliability and to reduce cost, in which rotor speed measurements are not available.

The control of ac drives are more complex than the control of dc drives and the complexity increases significantly if high performance is demanded. The main causes for this complexity are the complex dynamics of ac motors, harmonically optimum converter power supplies, motor parameter variations, difficulty in processing feedback signals in the presence of harmonics and the need of variable frequency. The drive for the motor control can be selected based on several factors such as:

- One, two or four quadrant drive,
- Torque, speed or position control in primary loop or outer loop,
- Single or multi motor drive,
- Range of speed control: Inclusion of zero speed and field weakening regions,
- Accuracy and response time,
- Robustness with parameter and load torque variations,
- Control with speed sensor or sensor less control,
- Type of front end converter,
- Reliability, cost, maintainability and efficiency consideration,
- And Power factor, line power supply and harmonics consideration.

Generally, the performance of the drive at high speed is satisfactory but its performance at low speed region is poor. In the research, mostly the methods are estimating rotor flux angle and parameter tuning in vector control. The control of induction drive is a vast subject and the technology has further advanced in recent years.

1.2 Scalar Control

It is a non-vector control scheme featured by only magnitude control. Its principle is to adjust constant Voltage to Frequency ratio of the stator voltage by feed forward control. Its purpose is to uphold the magnetic flux in the machine at a required level. It is a very simple method of speed control for motor drives. Its simplicity satisfies only moderate dynamic requirements. The speed of the motor can be controlled by changing the magnitude of voltage or frequency of the induction motor. The air gap flux can be controlled by the voltage and the frequency and is used to control the torque. As the flux and torque are both functions of frequency and voltage respectively, so, there exist the coupling effect between the flux and torque, which degrades the performance of the scalar control. The dynamic performance of the scalar control can be used for small variation of motor speed and load. But for high performance drives, its performance is not satisfactory.

Scalar control guarantees robustness at the cost of reduced dynamic performance which is sufficient for some applications like pump and fan drives and acceptable for other applications if budget is a concern. The absence of the closed loop control and the constraint of low dynamic performance make the drive robust. They operate stable even in the very low speed region where the field oriented control fails to maintain stability. Open loop control is a benefit for very high speed applications like centrifuges and grinders since the current control system of closed loop scheme destabilises when operated at 5 to 10 times the nominal frequency of 50 or 60 Hz due to phase displacement in motion induced voltage.

The particular attraction of scalar controlled drives is their extremely simple control structure which favours an implementation by a few highly integrated electronic components. The cost saving characteristics are specifically essential for applications at low power below 5kW. At higher power, the power components themselves dominate the system budget, letting the implementation of more sophisticated control methods. Their purpose is to overcome the major limitation of scalar control that is the reduced dynamic performance. Still the cost advantage makes scalar control very attractive for low power applications and their robustness favours its use for high power applications when a fast response is not necessary. Therefore, such systems contribute a substantial share of the market for sensor less ac drives.

1.3 Vector Control

The principle of field orientation for high performance control of AC machines was developed in Germany in the late sixties and earlier seventies. Its principle is that the torque and machine flux are controlled independently similar to a separately excited DC machine. The field oriented control decouples the torque and flux producing components of stator currents of an induction machine and make them orthogonal like that of a separately excited dc machine, where the commutator does the above purpose. The stator current is resolved into two orthogonal components: one in the direction of flux linkage which represents the magnetizing current or flux component of current and the other perpendicular to it, representing the torque component of current. Both the components are controlled independently. The two possible methods for achieving field orientation are; direct flux orientation where the field orientation is achieved by direct measurement or estimation of the flux, and indirect field orientation where the field orientation is achieved by imposing slip frequency derived from the rotor dynamic equations.

In field oriented control, high dynamic performance of variable speed AC drives is possible equalling that of the separately excited DC motor. Vector control or field oriented control is a method in which input currents of the motor are adjusted to set a specific angle in between. The key to vector control is the knowledge of rotor flux position angle with respect to the stator. The vector control methods in which rotor flux is sensed by flux sensing coils or it is calculated by motor terminal voltages and currents are generally called "direct vector control" methods. It is also possible to calculate the rotor flux angle from shaft position information, provided other motor parameters are known. This approach is generally called "indirect vector control". The indirect vector control eliminates the need for a flux sensor or flux model but it requires an accurate measurement of shaft position to determine the accurate location of the rotor flux vector.

1.4 Vector Control without Speed or Position Encoder

The use of induction drives with vector control provide a number of benefits over DC drives in terms of robustness, lack of brushes, size, reduced cost and maintenance. But induction motor drives require a precise shaft encoder for correct operation. The use of this encoder involves additional electronics. Extra space, extra wiring and careful mounting detracts cage induction motors from their inherent robustness. In addition at low powers (2 to 5kW) the cost of the encoder is about the same as the machine. Even at 50kW, it can still be between 20 to 30% of the motor cost. As a result there has been a great interest in the research community in developing a high performance induction drive that doesn't need a speed or position encoder for its operation.

To perform the speed control for high performance motor drives without any speed or position encoder, some kind of speed estimation is necessary. Speed can be estimated from terminal quantities either by using a machine model or by exploiting magnetic saliencies in the machine. Speed estimation using magnetic saliencies such as rotor asymmetries, rotor slotting or variations on leakage reactance is independent of motor parameters and can be considered as true speed measurement. But some of these approaches require specially modified machines or injection of disturbance signals. Usually, these methods can't be used directly as speed feedback signal for high performance speed control. Because they present relative large measurement delays and they can only be used within a reduced range of frequencies.

On the other hand, the speed information can be estimated by using a machine model fed by stator quantities. These techniques use simple open loop speed calculators, Extended Kalman Filters and Model Reference Adaptive Systems (MRAS). All these methods are parameter dependant, as a result parameter errors can degrade the speed holding characteristics. In some cases parameter errors can also cause dynamic oscillations. But these methods provide fast speed estimation. So they are suitable for direct use for speed feedback.

The common problems of the speed estimation are:

- **Parameter sensitivity**: One of the main concerns of the sensor less control algorithms for the vector controlled induction drive is the insufficient information about the motor parameters which yields the estimation of some motor parameters along with the sensor less structure. Among these parameters, stator resistance, rotor resistance and rotor time constant play more significant role than the other parameters as these values are more sensitive to temperature variations. The knowledge of the exact stator resistance R_s is essential to widen the operation region towards the lower speed range. As the induced voltage is low at low speeds and stator resistance voltage drop becomes dominant, mismatch of stator resistance makes the system unstable. Alternatively, errors made in calculating the actual value of the rotor resistance R_r may cause the instability of the system.

- **Pure Integration**: The other significant issue regarding many of the speed estimating topologies is the integration process inherited from the dynamics of induction machine where an integration process is required to determine the state variables of the system. On the other hand, it is difficult to determine the initial value and prevent the drift of the output of pure integrator. Generally, low pass filters replace the integrators to overcome this issue.

1.5 Overview of the Chapters

Chapter 2 presents the modelling of the induction machine with stationary reference frame. The simulation of the model is implemented by using Matlab – Simulink. The simulation model and results are presented. The torque and speed responses are observed with the application of sudden load torque.

Chapter 3 presents the detailed study of indirect vector control of induction motor. In addition to the studies, the simulation of the model is implemented by using Matlab – Simulink. The simulation results are presented for both no load and loaded conditions. The steady state and dynamic performances of the system have been observed with step change in reference speed and sudden change in load.

Chapter 4 presents the sensor less control of induction motor with rotor flux, back emf and instantaneous reactive power based MRAS speed estimation techniques. The Matlab – Simulink model and the results are presented under no load and loaded conditions with particular focus on low speed operation. The effect of parameter variations is observed for all the estimation schemes.

Chapter 5 presents the practical implementation of the sensor less vector control of induction drive with reactive power based MRAS scheme. The results are presented with various conditions and the effect of parameter variations is also observed.

2. INDUCTION MACHINE MODELLING

2.1 Introduction

To control any power electronic drive such as an induction drive, controllers have to be designed for controlling the system. As the systems are having higher order nonlinearity and multivariable nature, mathematical modelling of the drive is required. The power electronics drive systems can be designed and developed by proper mathematical modelling of the plant. The modelling of the induction motor is done by three phase (abc) to two phase (dq) transformation by making the following assumptions:

- ➢ Space harmonics of the stator magnetic flux and the rotor magnetic flux are neglected
- ➢ Geometrical configuration and the electrical configuration of the motor is symmetrical
- ➢ Infinite permeable iron
- ➢ Slotting effect and the saliency effect are negligible
- ➢ Stator winding and the rotor winding are distributed sinusoidally in space and replaced by an equivalent concentrated winding
- ➢ Core loss, magnetic saturation, skin effect and anisotropy effect are neglected
- ➢ Voltage and current are sinusoidal terms
- ➢ Winding resistance and winding reactance don't vary with temperature
- ➢ End effect and fringing effect are negligible

In this chapter, modelling of the induction motor and the simulated results have been discussed. The nonlinear dynamics of the induction motor are represented by a set of differential equations in a stationary d-q reference frame with the stator voltages and load torque as the input variables and the electromagnetic torque developed and the rotor angular velocity as the output variables.

2.2 Induction Motor Modelling

The stator and rotor voltage equations of the three phase induction motor in a stationary reference frame are given below:

$$V_{ds} = R_s i_{ds} + \frac{d\Psi_{ds}}{dt} \tag{2.1a}$$

$$V_{qs} = R_s i_{qs} + \frac{d\Psi_{qs}}{dt} \tag{2.1b}$$

$$V_{dr} = R_r i_{dr} + \frac{d\Psi_{dr}}{dt} + T_e \Psi_{qr} \tag{2.1c}$$

$$V_{qr} = R_r i_{qr} + \frac{d\Psi_{qr}}{dt} - \omega_r \Psi_{dr} \tag{2.1d}$$

The electromagnetic torque developed T_e is given by;

$$T_e = \frac{3P}{4} (\Psi_{ds} i_{qs} - \Psi_{qs} i_{ds}) \tag{2.1e}$$

The torque balancing equation is given by;

$$T_e = T_L + \beta \omega_m + J \frac{d\omega_m}{dt} \tag{2.1f}$$

Where

V_{ds}, V_{qs} are stator d axis and q axis voltages in V

V_{dr}, V_{qr} are rotor d axis and q axis voltages in V

i_{ds}, i_{qs} are stator d axis and q axis currents in A

i_{dr}, i_{qr} are rotor d axis and q axis currents in A

ω_m is rotor mechanical speed in rad/s

ω_r is rotor electrical speed in rad/s

R_s, R_r are stator and rotor per phase resistances in ohms (Ω)

Ψ_{dr}, Ψ_{qr} are rotor d axis and q axis flux linkages in V.s

Ψ_{ds}, Ψ_{qs} are stator d axis and q axis flux linkages in V.s

P is no. of poles

J is moment of inertia in kg.m^2

β is coefficient of viscous friction in N.m.s./rad

T_e is torque developed in N.m.

T_L is load torque in N.m.

The stator and rotor voltage equations and the electromagnetic torque equations can be represented in matrix form as given below;

$$\begin{bmatrix} V_{ds} \\ V_{qs} \end{bmatrix} = \begin{bmatrix} R_s & 0 \\ 0 & R_s \end{bmatrix} \begin{bmatrix} i_{ds} \\ i_{qs} \end{bmatrix} + \frac{d}{dt} \begin{bmatrix} \Psi_{ds} \\ \Psi_{qs} \end{bmatrix} \tag{2.2}$$

$$\begin{bmatrix} V_{dr} \\ V_{qr} \end{bmatrix} = \begin{bmatrix} R_r & 0 \\ 0 & R_r \end{bmatrix} \begin{bmatrix} i_{dr} \\ i_{qr} \end{bmatrix} + \frac{d}{dt} \begin{bmatrix} \Psi_{dr} \\ \Psi_{qr} \end{bmatrix} + \begin{bmatrix} 0 & \omega_r \\ -\omega_r & 0 \end{bmatrix} \begin{bmatrix} \Psi_{dr} \\ \Psi_{qr} \end{bmatrix} \tag{2.3}$$

$$T_e = \frac{3P}{4} \begin{bmatrix} \Psi_{ds} & \Psi_{qs} \end{bmatrix} \begin{bmatrix} i_{qs} \\ -i_{ds} \end{bmatrix} \tag{2.4}$$

The rotor windings of the induction motor are short circuited, so $V_{dr} = V_{qr} = 0$.

Let L_s, L_r are stator and rotor self inductances respectively and L_m is the mutual inductance between stator and rotor

So, neglecting the magnetic saturation of the circuit and iron losses, the flux linkage equations of the circuit can be represented in matrix form as given below;

$$\begin{bmatrix} \Psi_{ds} \\ \Psi_{qs} \end{bmatrix} = \begin{bmatrix} L_s & 0 \\ 0 & L_s \end{bmatrix} \begin{bmatrix} i_{ds} \\ i_{qs} \end{bmatrix} + \begin{bmatrix} L_m & 0 \\ 0 & L_m \end{bmatrix} \begin{bmatrix} i_{dr} \\ i_{qr} \end{bmatrix} \tag{2.5a}$$

$$\begin{bmatrix} \Psi_{dr} \\ \Psi_{qr} \end{bmatrix} = \begin{bmatrix} L_r & 0 \\ 0 & L_r \end{bmatrix} \begin{bmatrix} i_{dr} \\ i_{qr} \end{bmatrix} + \begin{bmatrix} L_m & 0 \\ 0 & L_m \end{bmatrix} \begin{bmatrix} i_{ds} \\ i_{qs} \end{bmatrix} \tag{2.5b}$$

By solving the equations (2.5a) and (2.5b), we get;

$$\begin{bmatrix} i_{ds} \\ i_{qs} \\ i_{dr} \\ i_{qr} \end{bmatrix} = \begin{bmatrix} \frac{L_r}{L_sL_r-L_m^2} & 0 & -\frac{L_m}{L_sL_r-L_m^2} & 0 \\ 0 & \frac{L_r}{L_sL_r-L_m^2} & 0 & -\frac{L_m}{L_sL_r-L_m^2} \\ -\frac{L_m}{L_sL_r-L_m^2} & 0 & \frac{L_s}{L_sL_r-L_m^2} & 0 \\ 0 & -\frac{L_m}{L_sL_r-L_m^2} & 0 & \frac{L_s}{L_sL_r-L_m^2} \end{bmatrix} \begin{bmatrix} \Psi_{ds} \\ \Psi_{qs} \\ \Psi_{dr} \\ \Psi_{qr} \end{bmatrix} \tag{2.6}$$

By neglecting coefficient of viscous friction,

$$\frac{d\omega_m}{dt} = \frac{T_e - T_L}{J} \tag{2.7}$$

$$\omega_r = \frac{P}{2} \omega_m \tag{2.8}$$

2.3 Results & Discussion

In this chapter, modelling of the induction motor in a stationary reference frame is done so that it can be utilised in implementing field oriented control technique and speed estimation techniques for the induction motor drive. The speed and torque responses can be observed by applying the proper input voltages to the motor model which can be obtained by using feedback information or direct open loop voltages.
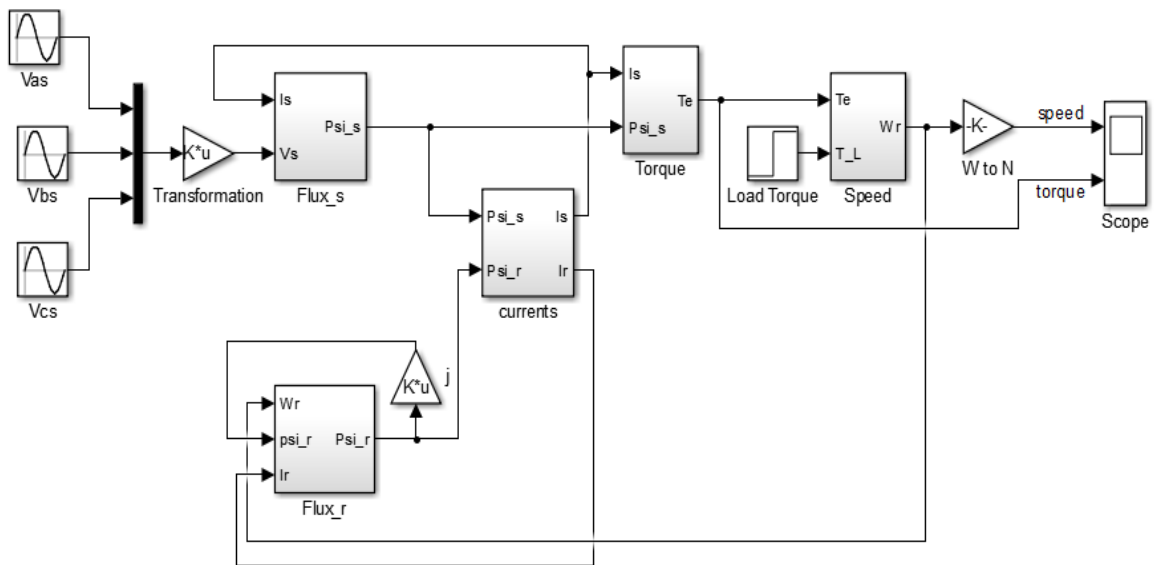
Fig.2.1 The Simulink model of IM
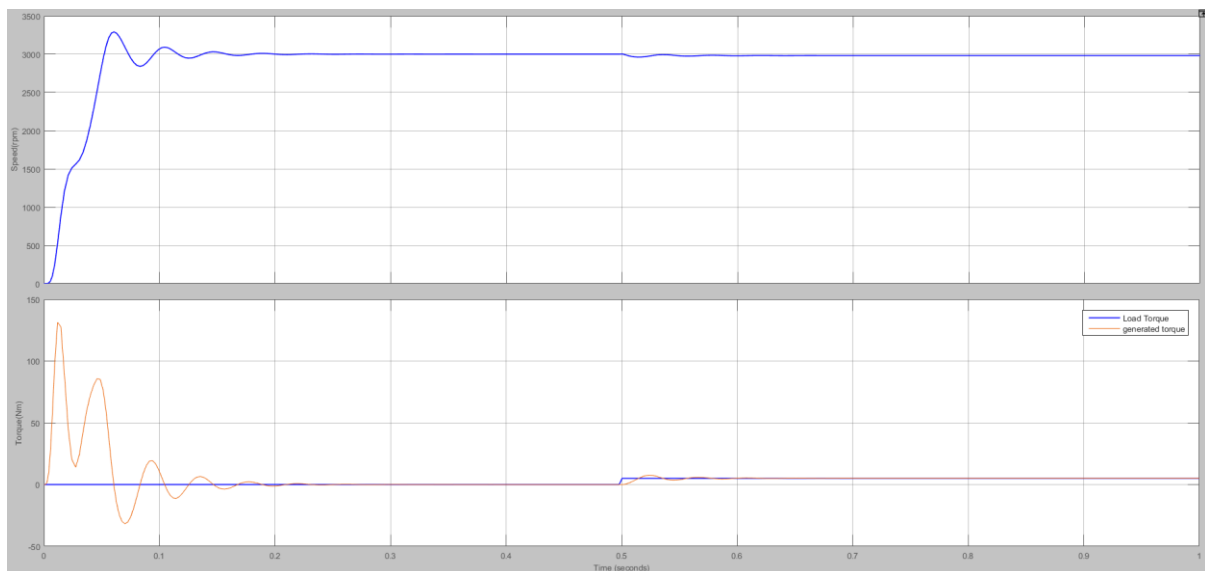
Fig.2.2 Simulation response of IM

Fig 2.1 shows the Simulink model of Induction Motor. Matlab - Simulink is used to implement the simulation. In the model, three phase voltages and load torque are the inputs whereas rotor speed and electro-mechanical torque are the outputs. Fig 2.2 shows the speed and torque waveforms. After giving the supply, speed of the IM reaches to the rated speed in 0.2 sec. The starting transient oscillations can be observed in the response. At 0.5 sec, a step change in load torque is applied. Accordingly the electromechanical torque is generated and the rotor speed is reduced.

2.4 Summary

In this chapter, induction motor is mathematically modelled in a stationary reference frame and the simulation results are presented. With the application of load torque, there is slight dip in the rotor speed as there is no speed control loop. So, in next chapter, we go for closed loop speed control of induction motor.

3. VECTOR CONTROL

3.1 Introduction

Traditionally only DC motors were used for high performance applications but with vector control technique, the induction motor drives came into consideration in high performance applications. With the vector control scheme, the induction motor can be controlled in the same way as the separately excited DC motor. Torque control of the induction motor is attained by controlling torque and flux current components of the stator current independently as in the separately excited DC motor. There are two basic ways of attaining field orientation: namely Direct and Indirect Field Orientation. The direct field oriented control method depends on the generation of unit vectors from the stator flux signals or air gap flux signals. The air gap flux signals can be obtained either directly or estimated from stator voltage signals and stator current signals. The components of the stator flux can be calculated directly from the stator signals. In this system, rotor speed isn't needed to obtain the rotor field angle information. In the indirect field oriented control method, the rotor field angle and the unit vector signals can be obtained indirectly by the summation of rotor speed and slip frequency.

Basic requirements for the field oriented control are the knowledge of two currents (if induction motor is star connected) and the rotor flux position information. Obtaining the appropriate rotor flux position is the primary requirement in the field oriented control. Indeed if there is any error in this variable, rotor flux isn't aligned with the d axis and the estimation of current components goes wrong. In induction motor, as the rotor speed and the rotor flux speed are not equal (there is a slip speed), a special method is required to calculate the rotor flux position (angle).

Thanks to field oriented control, it is possible to control the flux and torque of the induction motor directly and separately. Vector controlled induction motor obtains every DC motor advantages such as instantaneous control of separate quantities permitting the precise transient as well as steady state management.

In DC machine, the armature flux and the field flux are perpendicular to each other. So these two fluxes do not produce net interaction on one another due to orthogonal nature. Consequently the DC machine flux can be controlled by adjusting the field current independently of torque and adjusting the armature current can control the torque independently of flux. In AC machine, there is an interaction between the stator field and the

rotor field. They are not perpendicular to each other and vary with the operating conditions. The performance similar to DC machine to hold a fixed and orthogonal orientation between the armature flux and the field flux can be obtained in an AC machine by orienting the stator current with respect to the rotor flux to achieve independent control of torque and flux. Such a control system is known as flux oriented control or vector control. And the vector control is also called an independent control or decoupled control.

The squirrel cage induction drive with the field oriented control or the vector control provides high dynamic performance. The closed loop control associated with the drive offers long term stability of the system. Induction drives are used in industrial and process control applications which require high performance. In high performance drive systems, the motor speed has to track a particular reference trajectory irrespective of parameter variations, load disturbances and model uncertainties. For achieving high performance, field oriented control of induction motor is implemented. The design of controller for such system plays a vital role in system performance. The decoupling characteristics of vector controlled induction motor are adversely affected by the parameter variations in the motor.

3.2 Indirect Vector Control

Field oriented control or vector control involves processing the stator currents in a definite coordinate system. Stator currents are time varying in nature when processed in stator coordinates and consequently the control system may produce an unwanted velocity error. Hence it is better to implement the current control in synchronous coordinates. Vector control method controls the voltage, frequency and phase as well whereas traditional methods for example scalar control method controls only the amplitude and frequency of the applied voltage. Field oriented control provides several advantages including high dynamic performance, speed control over wide range, accurate speed regulation and operation above base speed. Rotor flux position can be obtained directly or indirectly. In the indirect vector control of induction motor, slip speed estimation is based on the measured or estimated rotor speed to calculate the synchronous speed of the motor, whereas in the direct vector control, the synchronous speed is computed with the aid of a flux estimator. Indirect vector control scheme controls the stator currents and slip frequency. Instantaneous torque can be controlled in the entire speed range with indirect vector control. The rotor flux is controlled with the help of d axis component of the stator current whereas the toque is controlled by using q axis component of the stator current and slip frequency.
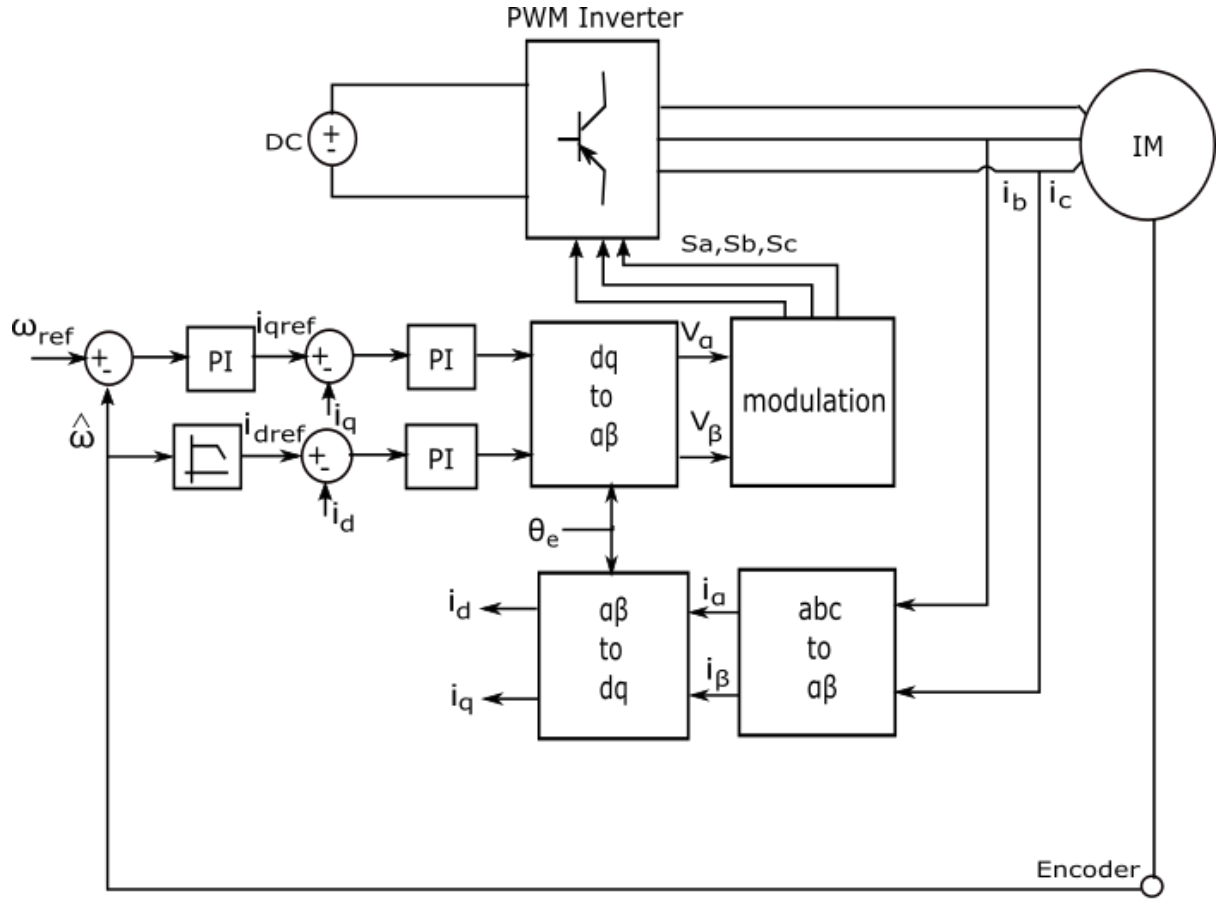
Fig.3.1 Vector Control of Induction Motor

The governing equations to implement Indirect Vector control scheme are given below:

$$\theta_e = \int \omega_e \, dt = \int (\omega_r + \omega_{sl}) \, dt \qquad (3.1)$$

The rotor side equations are given by;

$$\frac{d}{dt}\Psi_{dr} + \frac{R_r}{L_r}\Psi_{dr} - \frac{L_m}{L_r}R_r i_{ds} - \omega_{sl}\Psi_{qr} = 0 \qquad (3.2a)$$

$$\frac{d}{dt}\Psi_{qr} + \frac{R_r}{L_r}\Psi_{qr} - \frac{L_m}{L_r}R_r i_{qs} - \omega_{sl}\Psi_{dr} = 0 \qquad (3.2b)$$

$$\Psi_r = \sqrt{\Psi_{qr}^2 + \Psi_{dr}^2} \qquad (3.3)$$

For decoupling control, the entire rotor flux is aligned along the d axis of synchronously rotating reference frame and hence

$$\Psi_{qr} = 0 \qquad (3.4a)$$

$$\Psi_{dr} = \Psi_r \qquad (3.4b)$$

14

By considering equation (3.4), the equation (3.2) can be modified as

$$\frac{L_r}{R_r}\frac{d}{dt}\overline{\Psi}_r + \overline{\Psi}_r = L_m i_{ds} \qquad (3.5)$$

Slip frequency is computed as

$$\omega_{sl} = \frac{i_{qs}}{\tau_r i_{ds}} \qquad (3.6)$$

The torque is given by

$$T_e = \frac{3P}{4}\frac{L_m}{L_r}\Psi_{dr}i_{qs} \qquad (3.7)$$

Where

θ_e is field angle in rad

ω_e is synchronous speed in rad/s

ω_r is rotor electrical speed in rad/s

ω_{sl} is electrical slip speed in rad/s

i_{ds}, i_{qs} are stator d axis and q axis currents in A

R_s, R_r are stator and rotor per phase resistances in ohms (Ω)

L_s, L_r are stator and rotor self inductances

L_m is the mutual inductance between stator and rotor

Ψ_{dr}, Ψ_{qr} are rotor d axis and q axis flux linkages in V.s

T_e is torque developed in N.m.

P is no. of poles

3.3 Results & Discussion

In this chapter, Indirect vector control of Induction motor drive is discussed thoroughly. Furthermore to the details regarding the theoretical models, the simulation of these models are employed by using Matlab – Simulink to check the theoretical results.
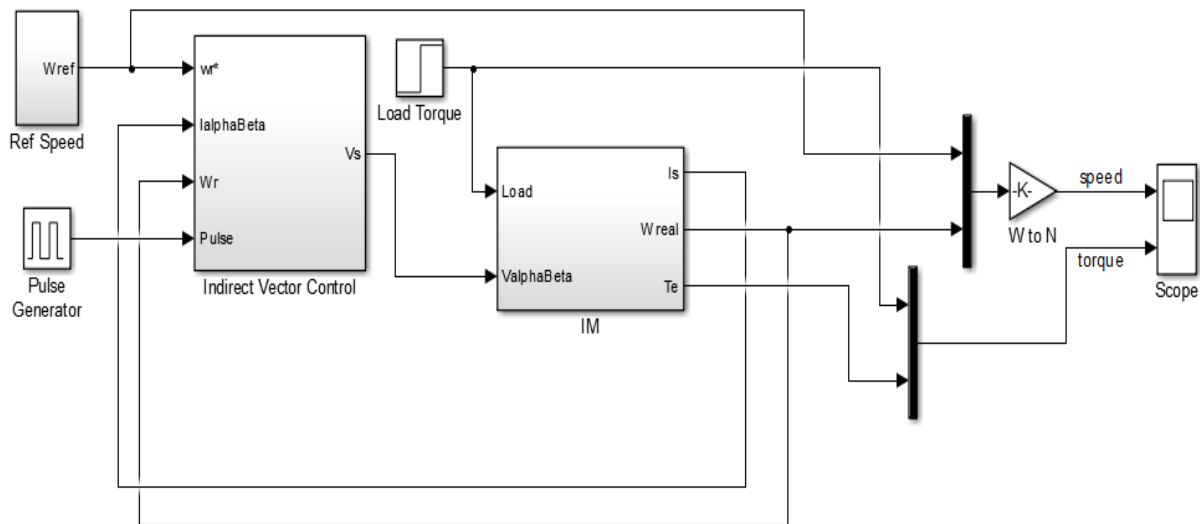
Fig.3.2 The Simulink model of FOC of IM

Fig 3.2 shows the Simulink model of Field Oriented Control of Induction Motor. The vector controlled induction motor drive is modelled with rotor flux and stator current components as state variables. PI controllers have been used for speed and torque control. PI controllers are designed by trial and error method. All this is achieved by making the system decoupled. The Simulink model of the Indirect Vector Control scheme is shown in Fig 3.3. Simulations have been carried out under both no load and loaded conditions.

Fig 3.4 shows the results acquired for the closed loop speed control of Induction Motor with Indirect Vector Control scheme under no load condition. Ref. speed and actual speed are presented in first segment with a step change of Ref. speed from 0 rpm to 100 rpm at 1 sec, 100 rpm to 0 rpm at 3 sec, 0 rpm to -100 rpm at 5 sec and -100 rpm to 0 rpm at 7 sec. At steady state, the actual speed measured reaches to the reference speed. Load torque and generated torque are shown in second segment.
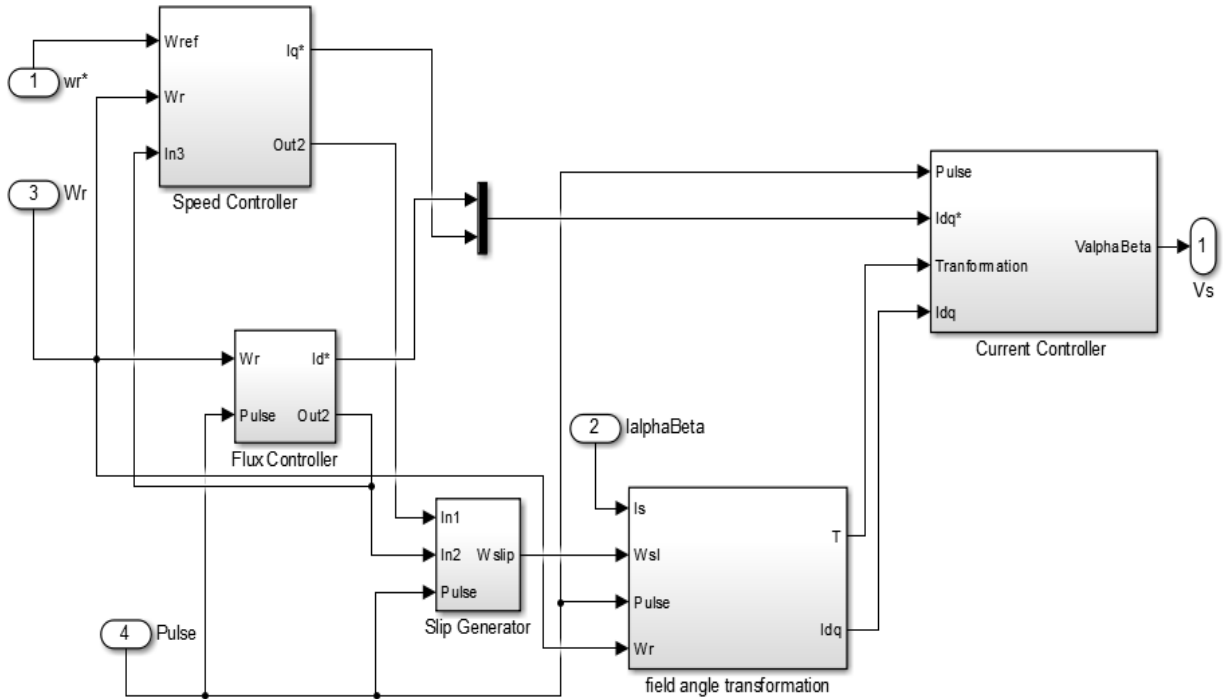
Fig.3.3 The Simulink model of Indirect vector control scheme

To study the performance of the system under loaded condition, step change in load torque is applied at 3 sec while maintaining Ref. speed at 50 rpm and a step change of reference speed from 50 rpm to 100 rpm is introduced at 5 sec while the load torque is at 5 Nm. Fig 3.5 represents the performance of the system under loaded condition. Reference speed and actual speed are shown in first segment. A momentary dip in the actual speed was observed when there is a sudden change in the load torque. The system stabilises and the actual speed reaches to the reference speed as showed in Fig 3.5. Load torque and generated torque are shown in second segment.
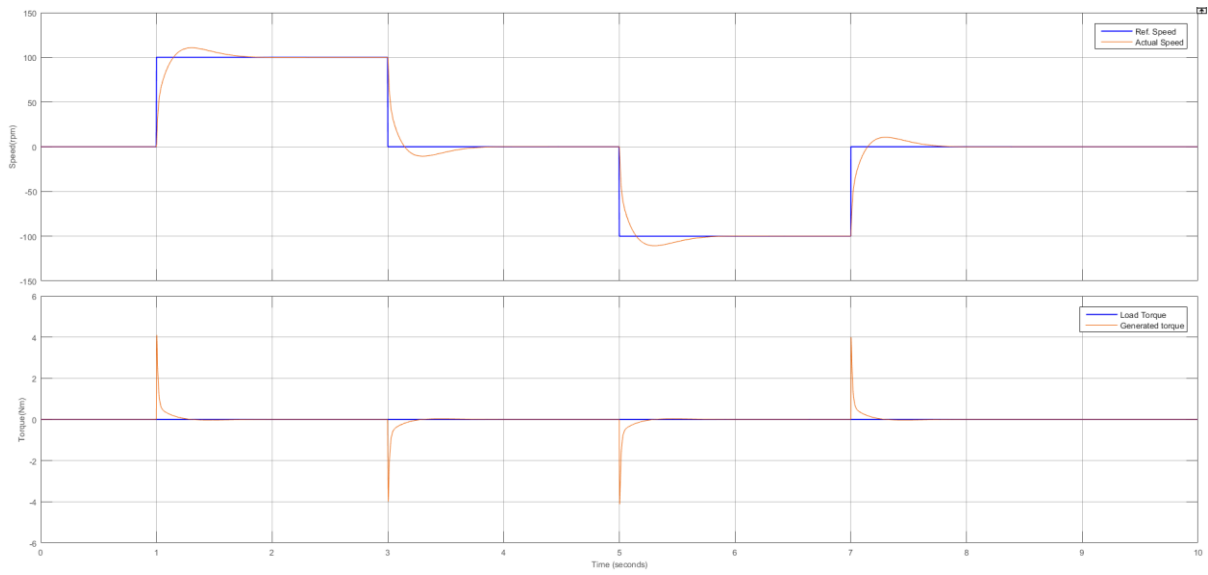
Fig.3.4 Simulation responses for No-load condition
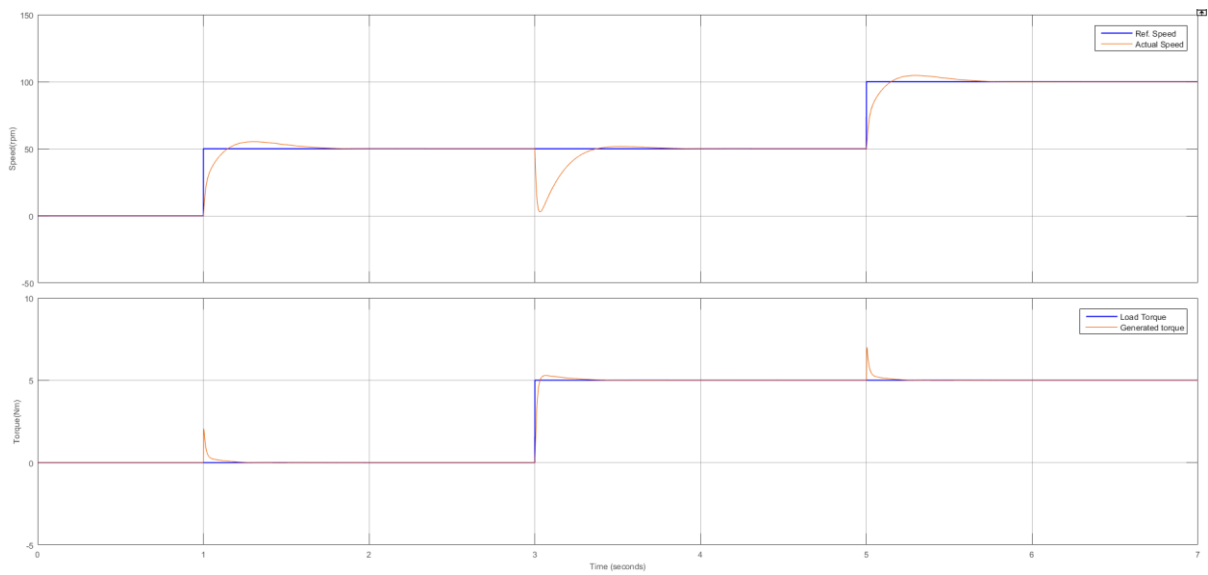
Fig.3.5 Simulation responses for Load condition

3.4 Summary

In this chapter, the indirect vector controlled induction motor with PI controller is simulated under both no load and loaded conditions. And the Steady state and Dynamic performances of the system are also witnessed. The system is stable with step change of ref. speed as well as with step change of load torque.

The system responses are studied and concluded that the speed response is sluggish as compared to that of the torque response and reached to the steady state slower than the torque response.

In Indirect Vector Control block, the speed from the Induction machine is used as feedback for speed control as well as rotor flux angle calculation. Practically this method requires a speed sensor such as shaft encoder. But the sensors used in electrical drive reduce the reliability of the systems particularly in hostile environment and need special attention to electric noise. So, in the next chapter, we go for sensor-less control of Induction Motor where some kind of speed estimation is required to perform speed control.

4. SENSOR-LESS CONTROL

4.1 Introduction

Sensors widely used in electrical drive reduce reliability of the systems particularly in hostile environment and need special attention to electric noise. Furthermore, it is problematic to mount sensor in some applications on top of extra expenditures involved. The induction drive without mechanical speed sensor has low cost, low size and high reliability. This has directed to the investigation in sensor-less control systems. The speed estimation is an important aspect of the field oriented control in the recent years.

Fig.4.1 Sensor-less Vector Control of Induction Machine

The rotor speed can be derived from the stator or rotor flux which is obtained by integrating the stator voltage equations in the stationary frame. This simple and basic technique suffers a

serious problem, especially in the low speed region, due to voltage measurement noise and integrator drift.

Numerous methods have been suggested previously for sensor less speed estimation for the control of induction machine. Most of the sensor-less speed estimation methods can be assembled into two groups, those are Fundamental wave model based and magnetic saliency based. Saliency based speed estimators utilise machine anisotropies such as rotor slotting or inductance saliency for estimating speed and the rotor position. This kind of estimator requires highly accurate measurements and hence increases complexity of the whole system. However the speed estimation using rotor saliency is more precise and independent of motor parameters. But they involve significant measurement delays and as a result can't be used for speed feedback.

Earlier the fundamental wave model based speed estimators processed open loop motor voltages and currents for estimating the rotor speed. Those methods were very sensitive to the motor parameter variations. Latest methods involve closed flux estimates for better dynamic performance and noise immunity. State observers like Luenberger observers and Kalman Filters assume Linear Time Invariant machine model for estimating the rotor speed. Enormous Real time calculations involved in these methods make them complex for implementing in Industry. Furthermore a precise knowledge of motor parameters is necessary for these estimators.

Model Reference Adaptive system (MRAS) techniques are the most popular and attractive adaptive control techniques to track and observe the system parameters and states because of their design simplicities. A precise estimate can be achieved by using MRAS method. An adaptive law should be defined for every MRAS technique such that the estimated values converge to the actual values and system becomes stable.

Fig.4.2 represents a general structure of MRAS system. It comprises of two motor models of different structures, those are Reference model and Adaptive model. MRAS principle is to observe and adjust the state variable of the system by using redundancy of two motor models with different inputs for estimating a quantity. The state variable of the system is represented as X in Fig.4.2. Reference model computes state variable by using a set of equations which doesn't involve the quantity to be estimated. Adaptive model observes the same state variable by using different set of input variables and equations which involve the quantity to be

estimated. Adaptive laws are formulated to ensure the stability of the system and for minimising the error between these two machine models.

Now we apply this MRAS scheme to the Induction motor to estimate the rotor speed with three different state variables which are rotor flux, back emf and instantaneous reactive power.
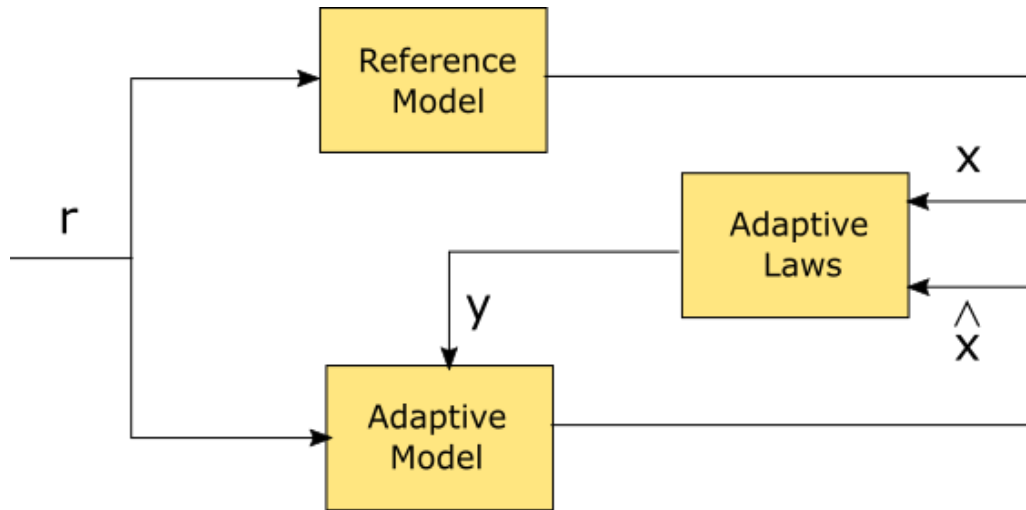
Fig.4.2 General Model of MRAS scheme

4.2 Rotor flux based MRAS speed estimation

The MRAS speed estimation scheme based on Rotor flux is originated from the point that both voltage model and current model of the motor can be used to calculate Rotor flux. The Rotor flux based MRAS scheme utilises motor voltage model to represent Reference model and motor current model to represent Adaptive model. The Rotor flux based MRAS speed estimator is represented in Fig.4.3.

Voltage model doesn't need rotor speed as one of its inputs to compute rotor flux. Current model utilises the rotor speed as one of its inputs for calculating the rotor flux. If we take the difference between the rotor fluxes calculated by these two models, an error vector can be generated. This error vector can be driven to zero by adjusting the parameter which can influence only the adaptive model. Output of the adaptive mechanism is rotor speed which is the estimated quantity.
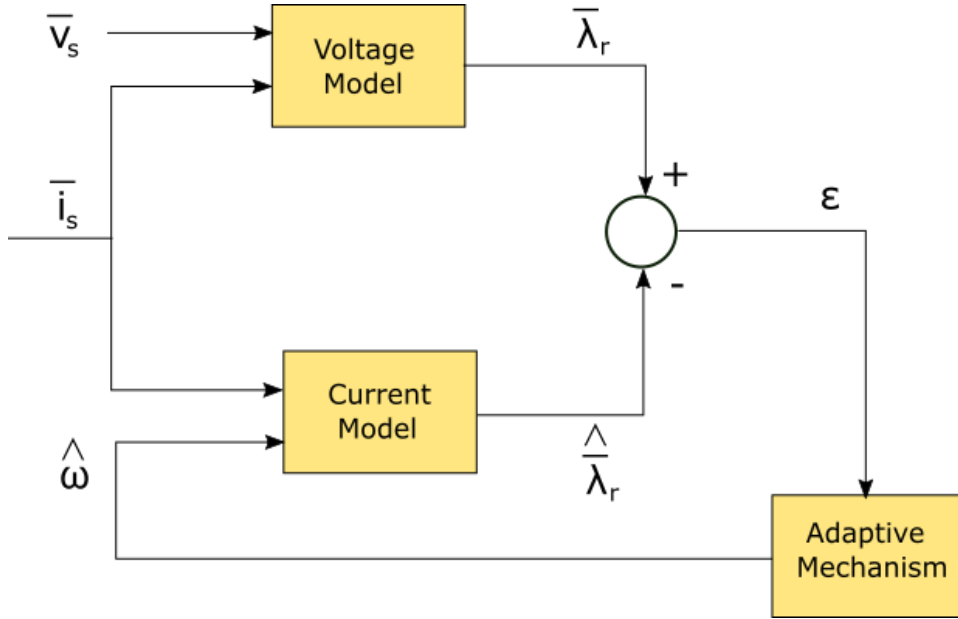
Fig.4.3 Rotor flux based MRAS observer

4.2.1 Voltage Model

The stator voltage of the induction motor is

$$\bar{v}_s = R_s \bar{\iota}_s + p\bar{\Psi}_s \tag{4.1}$$

where *p* is rate of change

$$\bar{\Psi}_s = L_{ls}\bar{\iota}_s + \bar{\Psi}_m \tag{4.2}$$
$$\bar{\Psi}_r = L_r\bar{\iota}_r + L_m\bar{\iota}_s \tag{4.3}$$
$$\bar{\Psi}_m = L_m(\bar{\iota}_s + \bar{\iota}_r) \tag{4.4}$$

By rearranging the above equations,

$$\bar{\Psi}_m = \frac{L_m\bar{\Psi}_r + L_{lr}L_m\bar{\iota}_s}{L_r} \tag{4.5}$$

From equations (4.1), (4.2) and (4.5)

$$\bar{v}_s = \frac{L_m}{L_r}p\bar{\Psi}_r + (R_s + \sigma L_s p)\bar{\iota}_s \tag{4.6}$$

Rewriting the equation (4.6) in dq coordinates gives the voltage model equations,

$$\Psi_{dr} = \frac{L_r}{L_m} \int \left[V_{ds} - (R_s + \sigma L_s p) i_{ds} \right] dt \qquad (4.7)$$

$$\Psi_{qr} = \frac{L_r}{L_m} \int \left[V_{qs} - (R_s + \sigma L_s p) i_{qs} \right] dt \qquad (4.8)$$

Where

$\bar{v}_s = \left[V_{ds}, V_{qs} \right]^T$, stator voltages

$\bar{\iota}_s = \left[i_{ds}, i_{qs} \right]^T$, stator currents

$\bar{\iota}_r = \left[i_{dr}, i_{qr} \right]^T$, rotor currents

$\overline{\Psi}_s = \left[\Psi_{ds}, \Psi_{qs} \right]^T$, stator flux linkages

$\overline{\Psi}_r = \left[\Psi_{dr}, \Psi_{qr} \right]^T$, rotor flux linkages

$\overline{\Psi}_m = \left[\Psi_{dm}, \Psi_{qm} \right]^T$, mutual flux linkages

4.2.2 Current Model

The short circuited rotor voltages are

$$R_r i_{dr} + p\widehat{\Psi}_{dr} + \widehat{\omega}_r \widehat{\Psi}_{qr} = 0 \qquad (4.9)$$

$$R_r i_{qr} + p\widehat{\Psi}_{qr} - \widehat{\omega}_r \widehat{\Psi}_{dr} = 0 \qquad (4.10)$$

Where $\widehat{\Psi}$ denotes estimated flux

Substituting the rotor current equations in terms of rotor flux and stator currents in the above equations and rearranging them yields the current model equations,

$$p\widehat{\Psi}_{dr} = -\widehat{\omega}_r \widehat{\Psi}_{qr} - \frac{1}{\tau_r} \widehat{\Psi}_{dr} + \frac{L_m}{\tau_r} i_{ds} \qquad (4.11)$$

$$p\widehat{\Psi}_{qr} = \widehat{\omega}_r \widehat{\Psi}_{dr} - \frac{1}{\tau_r} \widehat{\Psi}_{qr} + \frac{L_m}{\tau_r} i_{qs} \qquad (4.12)$$

It can be seen that rotor flux quantities can be calculated using the stator equations (which utilise measured stator voltages and currents, parameters and is called the 'voltage model') as

well as the rotor equations (which utilise measured stator currents, parameters and rotor speed and is called the 'current model').

In this estimator, an open loop integration is required to calculate the flux in Reference Model (Voltage Model). This pure integration is very problematic to implement due to DC drift and initial conditions. Replacing the integrator with Low Pass filter helps up to some extent but the estimation of flux deteriorates beneath cut-off frequency of the filter. On the other hand parameter sensitivity is one more limitation associated with this estimation scheme. As the Voltage model is derived based on motor parameters, this MRAS estimator which is based on Rotor Flux is very sensitive to parameter variations. The most severe problem is the variation of stator resistance with temperature especially near low speed region. At low speeds, the resistance drop and the applied voltage are almost equal as the stator voltage is low. Consequently it is very hard to maintain the stability near low speed region.

4.3 Back EMF based MRAS speed estimation

This MRAS scheme provides development to the rotor flux based MRAS speed estimation scheme. The back EMF based MRAS speed estimation doesn't need open loop integration in either reference model or adaptive model. For this type of estimator, the output of the two dynamic models is induced emf. Fig.4.4 represents the Back EMF based MRAS observer.
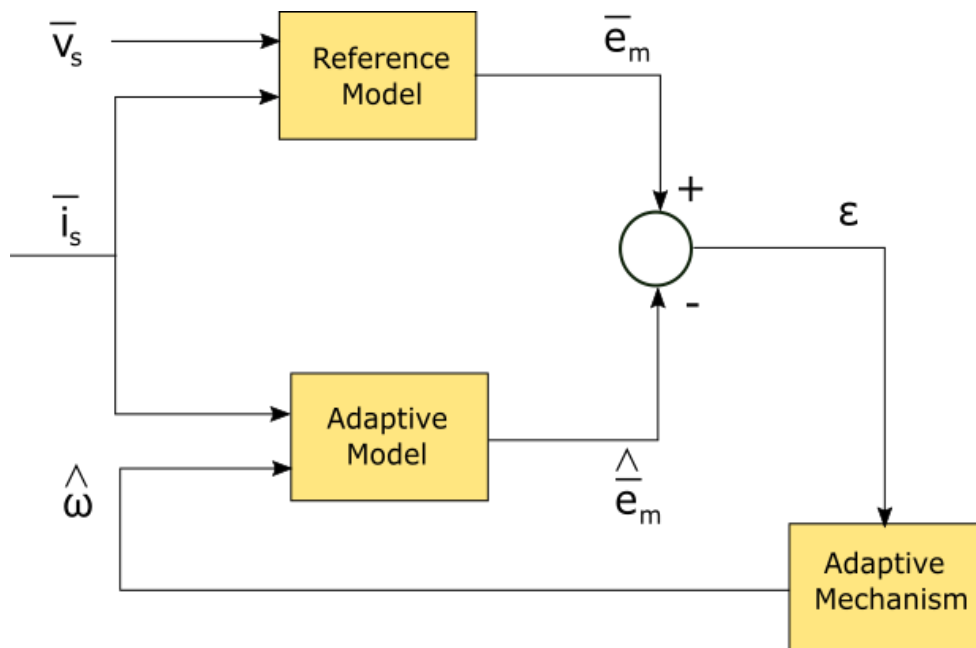

Fig.4.4 Back EMF based MRAS observer

Reference model doesn't need rotor speed as one of its inputs to compute back emf. Adaptive model utilises the rotor speed as one of its inputs for calculating the back emf. If we take the difference between the back emfs calculated by these two models, an error vector can be generated. This error vector can be driven to zero by adjusting the parameter which can influence only the adaptive model. Output of the adaptive mechanism is rotor speed which is the estimated quantity.

4.3.1 Reference Model

The induction motor back emf equations can be written from motor voltage model and given as below:

$$e_{md} = V_{ds} - (R_s + \sigma L_s p)i_{ds} \tag{4.13}$$

$$e_{mq} = V_{qs} - (R_s + \sigma L_s p)i_{qs} \tag{4.14}$$

4.3.2 Adjustable Model

$$\hat{e}_{md} = \frac{L_m^2}{L_r}\left(\frac{di_{md}}{dt}\right) \tag{4.15}$$

$$\hat{e}_{mq} = \frac{L_m^2}{L_r}\left(\frac{di_{mq}}{dt}\right) \tag{4.16}$$

Where

$$\frac{di_{md}}{dt} = -\widehat{\omega}_r i_{mq} - \frac{1}{\tau_r}i_{md} + \frac{1}{\tau_r}i_{ds} \tag{4.17}$$

$$\frac{di_{mq}}{dt} = -\widehat{\omega}_r i_{md} - \frac{1}{\tau_r}i_{mq} + \frac{1}{\tau_r}i_{qs} \tag{4.18}$$

$\tau_r = \frac{L_r}{R_r}$, rotor time constant

$\sigma = 1 - \frac{L_m^2}{L_s L_r}$, leakage factor

R_s, R_r are Stator and rotor per phase resistances in ohms (Ω)

L_s, L_r are stator and rotor self inductances

L_m is the mutual inductance between stator and rotor

It is obvious that no open loop integration or pure integration is required in either Reference model or Adaptive model. But the reference model is still dependant on stator resistance. The most severe problem is the variation of stator resistance with temperature especially near low speed region. At low speeds, the resistance drop and the applied voltage are almost equal as the stator voltage is low. Consequently it is very hard to maintain the stability near low speed region.

4.4 Reactive power based MRAS speed estimation

This MRAS scheme which is based on instantaneous reactive power is advantageous over those two schemes as this estimator does not have integrator drift problem which is one of the limitations in the rotor flux based MRAS speed estimator and sensitivity towards the stator resistance variation which is the common problem in both the Rotor flux based MRAS scheme and Back EMF based MRAS scheme. The Reactive power based MRAS speed estimator is represented in Fig.4.5.

Fig.4.5 Instantaneous Reactive power based MRAS observer
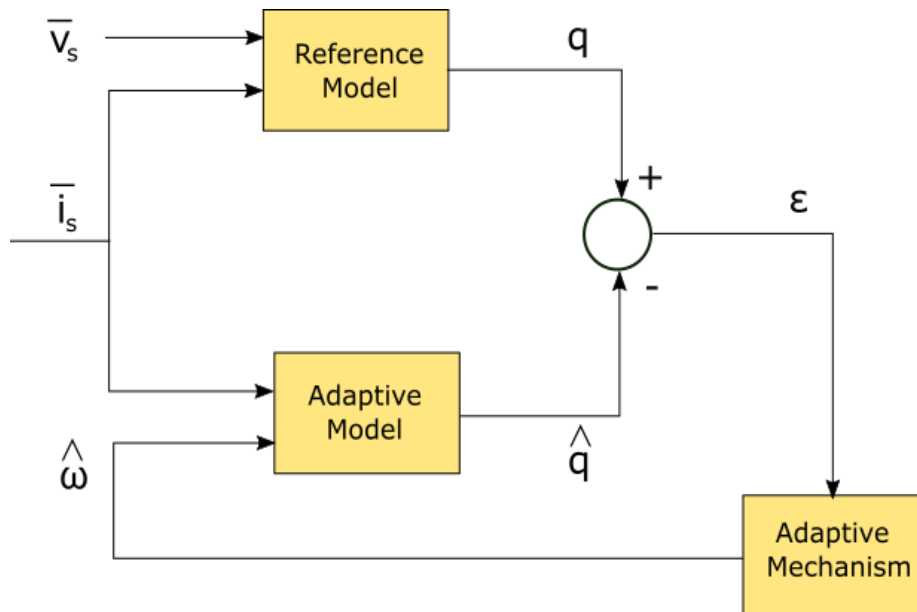
Reference model doesn't need rotor speed as one of its inputs to compute reactive power. Adaptive model utilises the rotor speed as one of its inputs for calculating the reactive power. If we take the difference between the reactive powers calculated by these two models, an error vector can be generated. This error vector can be driven to zero by adjusting the parameter

which can influence only the adaptive model. Output of the adaptive mechanism is rotor speed which is the estimated quantity.

4.4.1 Reference Model

Instantaneous reactive power can be obtained by taking cross product between back emf vector and stator current vector.

$$q = \bar{\imath}_s \circledast \bar{e}_m \tag{4.19}$$

Where

$$\bar{e}_m = \bar{v}_s - R_s\bar{\imath}_s - \sigma L_s p\bar{\imath}_s \tag{4.20}$$

From Equations (4.19) and (4.20), Reference model is realized as

$$q = \bar{\imath}_s \circledast \bar{v}_s - \sigma L_s(\bar{\imath}_s \circledast p\bar{\imath}_s) \tag{4.21}$$

It is evident that the reference model is not dependant on the stator resistance.

4.4.2 Adaptive Model

Adaptive model is deduced from the rotor side of the induction motor.

$$\hat{\bar{e}}_m = \frac{L_m}{L_r} p\widehat{\bar{\Psi}}_r \tag{4.22}$$

Rotor flux is formulated as

$$p\widehat{\bar{\Psi}}_r = \frac{L_m}{\tau_r}\bar{\imath}_s - \frac{1}{\tau_r}\widehat{\bar{\Psi}}_r + \hat{\omega}_r j\widehat{\bar{\Psi}}_r \tag{4.23}$$

From the equations (4.19), (4.22) and (4.23), instantaneous reactive power can be given by

$$\hat{q} = \frac{L_m}{L_r}\left[\frac{1}{\tau_r}\left(\widehat{\bar{\Psi}}_r \circledast \bar{\imath}_s\right) + \hat{\omega}_r\left(\bar{\imath}_s \circledast j\widehat{\bar{\Psi}}_r\right)\right] \tag{4.24}$$

Equations (4.21) and (4.24) structures the MRAS speed estimation scheme which is based on the instantaneous reactive power.

This method appears particularly attractive as it removes dependency on the stator resistance. In addition the estimator doesn't utilise integrators (or low pass filters acting as semi

integrators). Therefore it provides considerable improvements to the accuracy of speed estimates, particularly at low speed.

4.5 Derivation of Adaption law

One of the main significant portion of the total estimation procedure is design of the adaption mechanism which determines the stability of the system. It makes sure that the estimated value converges to the actual quantity with appropriate dynamic characteristics.

Adaptation Law is nothing but developing a set of instructions to ensure the system stability as well as to make the estimated value converges to the actual quantity. Adaptation law can be designed by using Popov's inequality criterion for hyper stability of time variant linear system. Now adaptive mechanism for the rotor flux based MRAS speed estimator is derived.

The following expressions are derived from the Equations (4.11) and (4.12) for Reference and Adaption models.

$$
p \begin{bmatrix} \Psi_{dr} \\ \Psi_{qr} \end{bmatrix} = \begin{bmatrix} -\frac{1}{\tau_r} & -\omega_r \\ \omega_r & -\frac{1}{\tau_r} \end{bmatrix} \begin{bmatrix} \Psi_{dr} \\ \Psi_{qr} \end{bmatrix} + \frac{L_m}{\tau_r} \begin{bmatrix} i_{ds} \\ i_{qs} \end{bmatrix}
\tag{4.25}
$$

$$
p \begin{bmatrix} \widehat{\Psi}_{dr} \\ \widehat{\Psi}_{qr} \end{bmatrix} = \begin{bmatrix} -\frac{1}{\tau_r} & -\widehat{\omega}_r \\ \widehat{\omega}_r & -\frac{1}{\tau_r} \end{bmatrix} \begin{bmatrix} \widehat{\Psi}_{dr} \\ \widehat{\Psi}_{qr} \end{bmatrix} + \frac{L_m}{\tau_r} \begin{bmatrix} i_{ds} \\ i_{qs} \end{bmatrix}
\tag{4.26}
$$

Defining a speed adaption signal,

$$
\varepsilon = \overline{\Psi}_r - \widehat{\overline{\Psi}}_r
$$

Subtracting (4.26) from (4.25),

$$
p \begin{bmatrix} \varepsilon_d \\ \varepsilon_q \end{bmatrix} = \begin{bmatrix} -\frac{1}{\tau_r} & -\widehat{\omega}_r \\ \widehat{\omega}_r & -\frac{1}{\tau_r} \end{bmatrix} \begin{bmatrix} \varepsilon_d \\ \varepsilon_q \end{bmatrix} + \begin{bmatrix} -\widehat{\Psi}_{qr} \\ \widehat{\Psi}_{dr} \end{bmatrix} (\omega_r - \widehat{\omega}_r)
\tag{4.27}
$$

That is,

$$
p[\varepsilon] = [A][\varepsilon] - [U]
\tag{4.28}
$$

Equation (4.28) denotes the nonLinear feedback system which is represented in Fig.4.6.
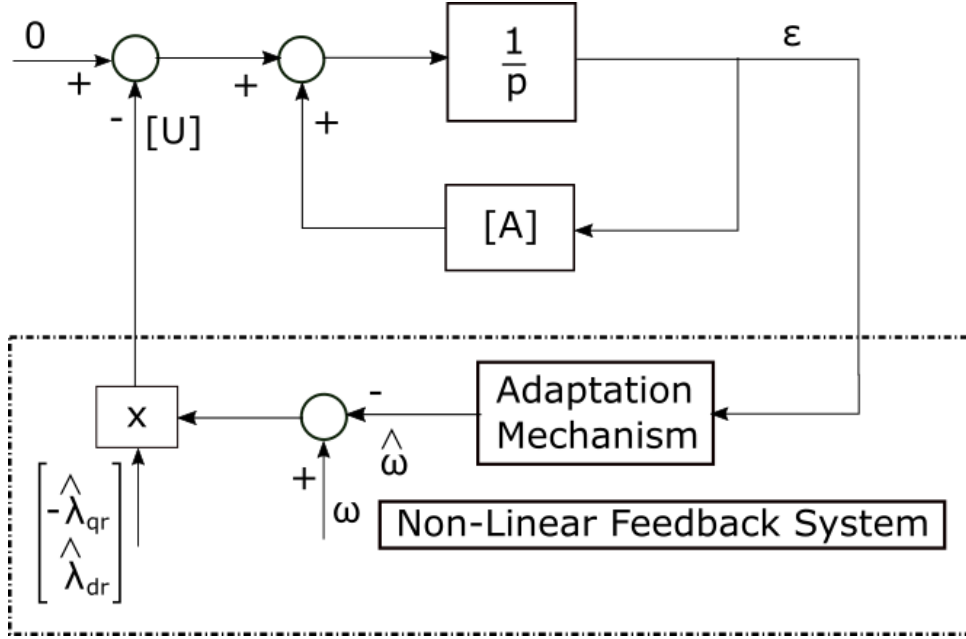
Fig.4.6 MRAS as NonLinear Feedback System

Hyper stability of the system shown in Fig.4.6 is certain only if forward path transfer matrix is positive real as well as nonLinear feedback system satisfies the Popov's inequality. Popov's inequality criterion says that a system can be asymptotically stable provided that inner product of the input and the output of the system is strictly negative integer constant. Therefore the stability conditions of the system shown in Fig.4.6 are

   i.   Feed forward transfer function $Z(s) = (sI - A)^{-1}$ is positive real.

   ii.   Popov's inequality Criterion

$$\int_0^{t1} [\mathcal{E}]^T [U] dt \geq -\gamma^2 \qquad \forall \ t \geq 0 \tag{4.29}$$

Where γ^2 is positive integer.

It can be proven that the transfer function is strictly positive by following Colin Schauder.

Let

$$\widehat{\omega}_r = \alpha([\mathcal{E}]) + \int_0^{t2} \beta([\mathcal{E}]) dt \tag{4.30}$$

Substituting for $[\mathcal{E}]$ and $[U]$ in Popov's criterion

$$\int_0^{t1} \left[-\mathcal{E}_d \widehat{\Psi}_{qr} + \mathcal{E}_q \widehat{\Psi}_{dr} \right] \left\{ \omega_r - \alpha(\mathcal{E}) - \int_0^{t2} \beta(\mathcal{E}) dt \right\} dt \geq -\gamma^2 \tag{4.31}$$

Following a well-known relation,

$$\int_0^t b\big(p.f(t)\big)f(t)dt \geq -\frac{1}{2}b[f(0)^2], b > 0 \tag{4.32}$$

The inequality (4.30) satisfies Popov's criterion if

$$\alpha = a1\big(\Psi_{qr}\widehat{\Psi}_{dr} - \Psi_{dr}\widehat{\Psi}_{qr}\big) \tag{4.33}$$

$$\beta = a2\big(\Psi_{qr}\widehat{\Psi}_{dr} - \Psi_{dr}\widehat{\Psi}_{qr}\big) \tag{4.34}$$

Thus from the definition of $\widehat{\omega}_r$, it can be seen that a PI controller having adaption signal Ɛ as its input outputs the estimated rotor speed.

4.6 Results & Discussion

In this chapter, rotor flux based, back emf based and instantaneous reactive power based MRAS speed estimation techniques are discussed thoroughly. Furthermore to the details regarding the theoretical models, the simulation of these schemes are employed by using Matlab – Simulink to check the theoretical results. In the simulation, the inputs for these MRAS schemes are the voltage and current of the induction motor. Two different and independent models are designed for computing the state space variables rotor flux, back emf and instantaneous reactive power. The structure that doesn't use estimated rotor speed as one of its inputs is the reference model and another structure which includes estimated rotor speed is the adjustable model or the adaptive model. The difference between these two outputs from the two models generates an error vector and it is fed to the adaptive mechanism that gives the estimated rotor speed which can be subsequently used as the input for adjustable model.
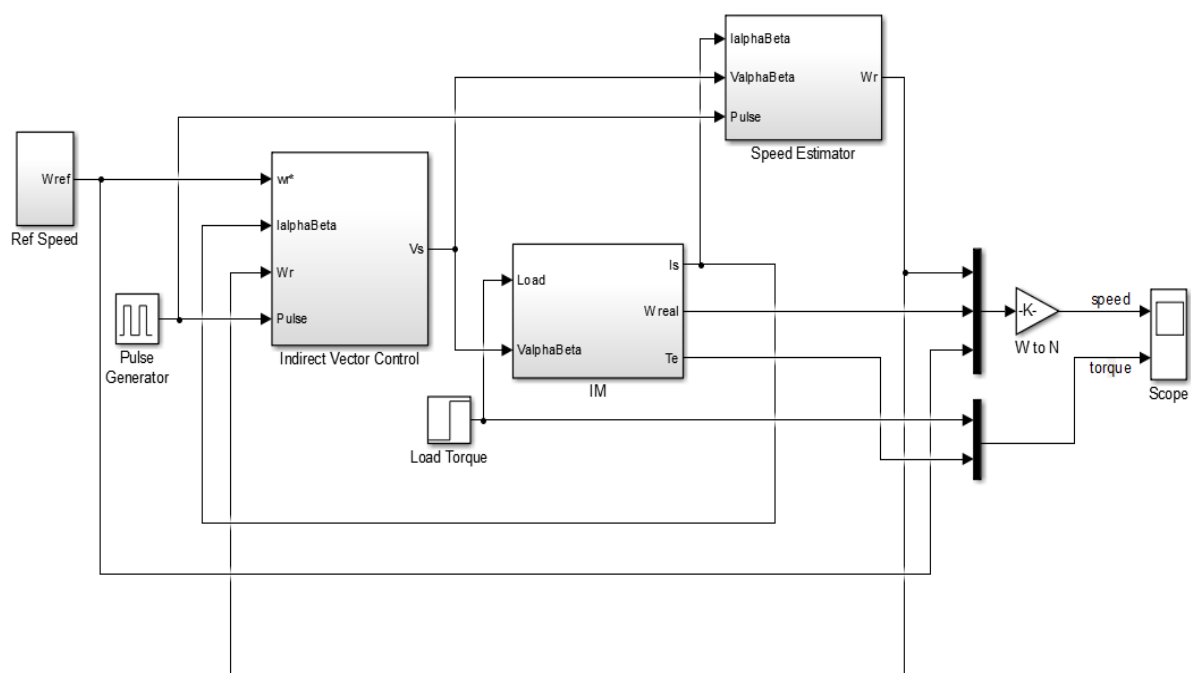
Fig.4.7 The Simulink model of FOC of IM with Speed Estimator

The estimated rotor speed from these MRAS methods is fed back to control the speed as well as to calculate the angle of rotor flux. The actual speed is sensed for observing the speed error (to validate MRAS schemes). Fig 4.7 shows the Simulink model of Induction machine with

Field Oriented Control by using the MRAS speed estimator. The simulation results of the three speed estimation techniques discussed above are presented here under different conditions.

4.6.1 Rotor flux MRAS scheme

Simulations are performed under no load condition as well as loaded condition. Fig 4.8 shows the Simulink model of Rotor flux MRAS scheme.
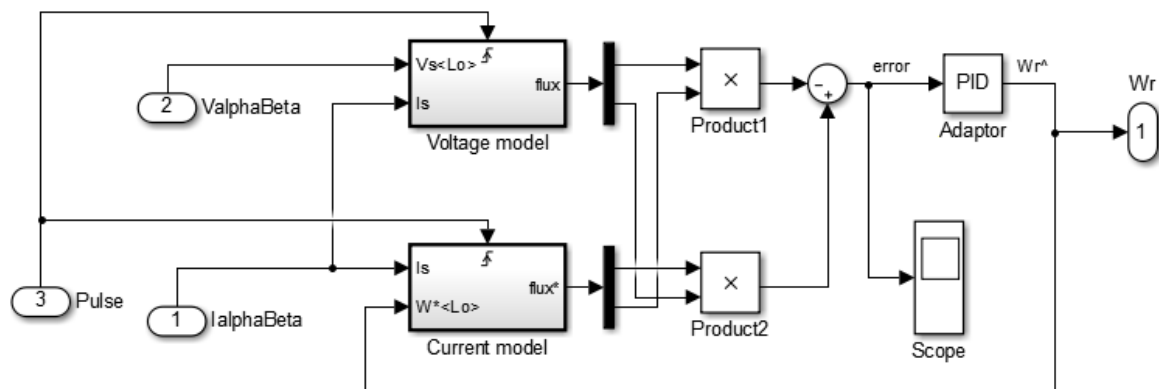

Fig.4.8 The Simulink model of Rotor flux MRAS scheme

Fig 4.9 presents performance of rotor flux MRAS method under no load condition. Ref. speed, actual measured rotor speed and the estimated rotor speed are presented in first segment. At steady state, the estimated rotor speed reaches the actual speed. Load torque and generated torque are shown in second segment. Adaption signal which is the difference between the rotor fluxes computed by the reference model and the adaptive model is shown in third segment.

 To observe the estimator's response under load, step change in load torque is applied at 3 sec by maintaining Reference speed at 50 rpm and a step change in Ref. speed is initiated at 5 sec while the load torque is at 5 Nm. Fig 4.10 represents the system's response under loaded condition. Ref. speed, actual measured rotor speed and the estimated rotor speed are presented in first segment. A momentary dip can be observed in both estimated and actual speeds with sudden application of the load. But the complete system gets stabilised and the estimated rotor speed reaches the measured speed as shown in Fig 4.10. Load torque and generated torque are shown in second segment. . Adaption signal which is the difference between the rotor fluxes computed by the reference model and the adaptive model is shown in third segment.
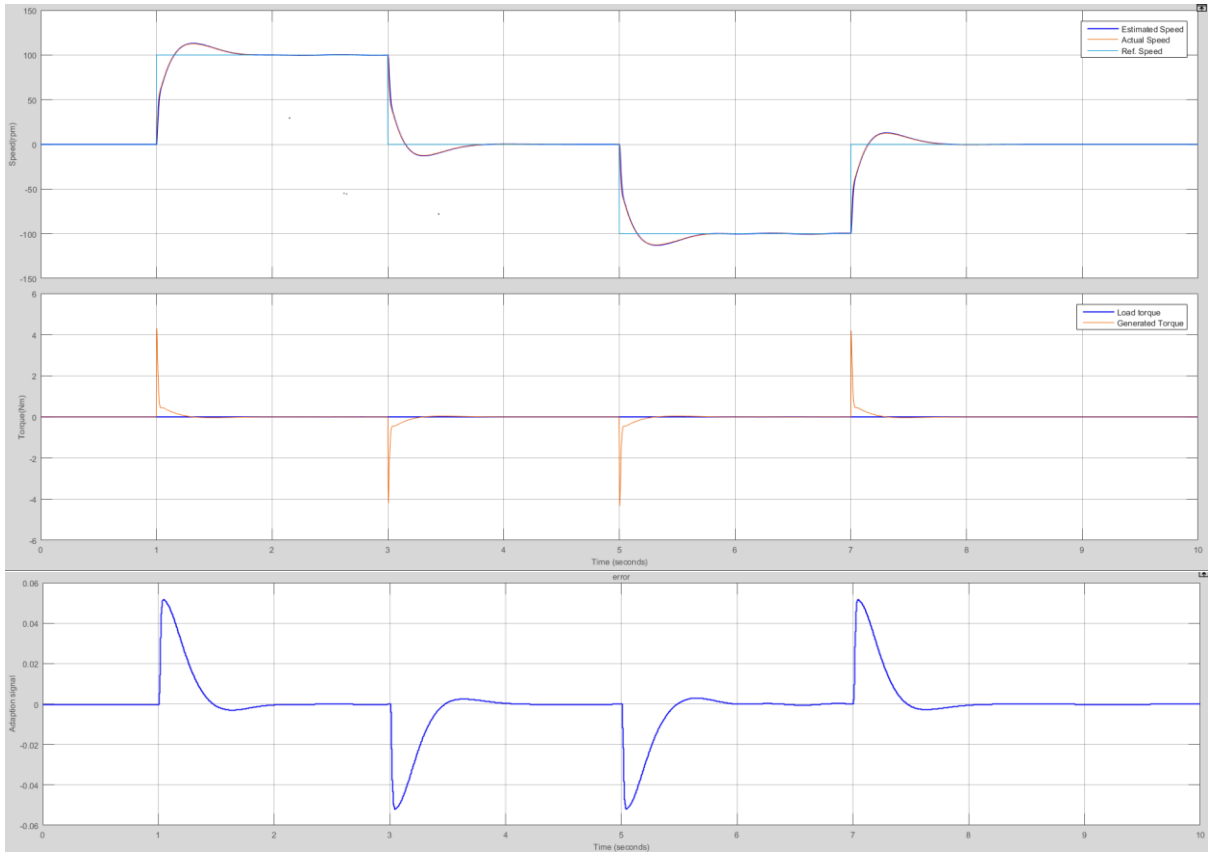
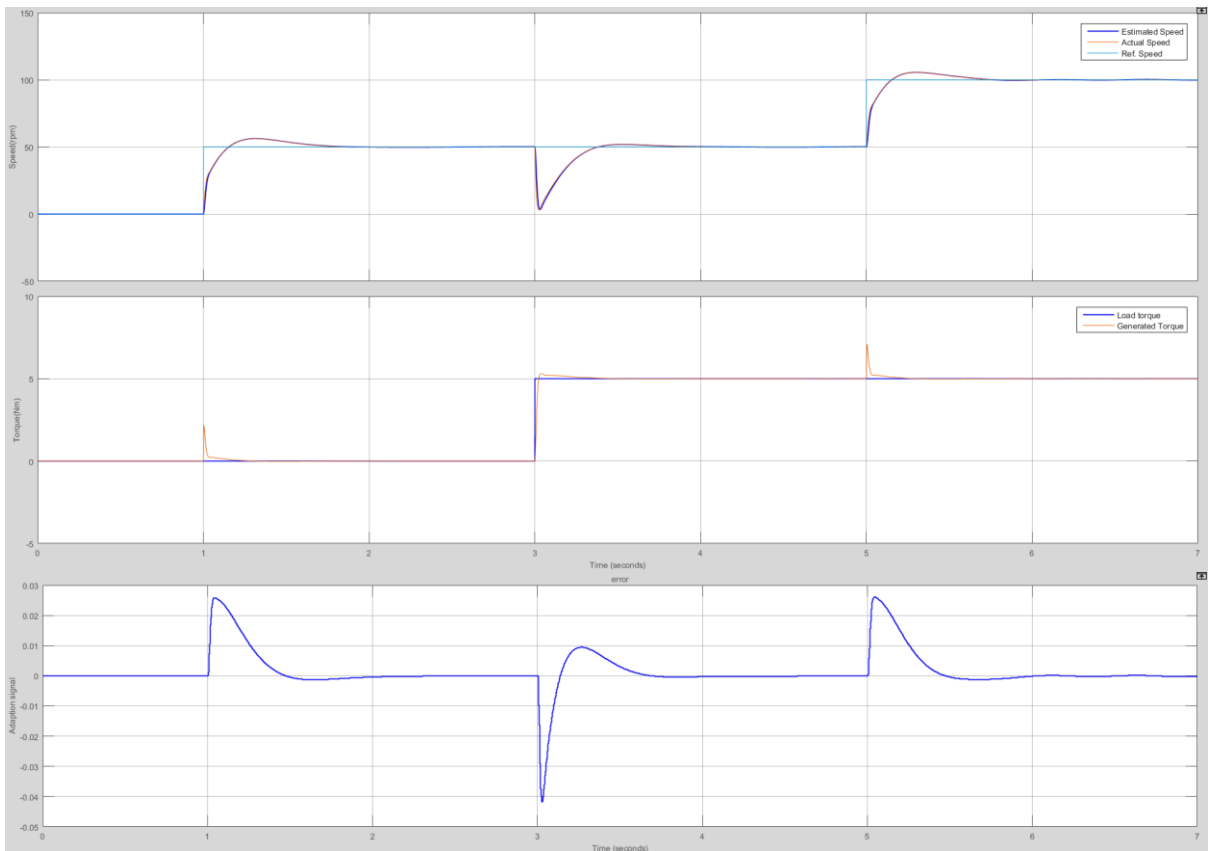Fig.4.9 Rotor flux MRAS Estimator Performance under No Load condition

Fig.4.10 Rotor flux MRAS Estimator Performance under Load condition

34

4.6.2 Back emf MRAS scheme

Similar to rotor flux estimation scheme, simulations are performed on Back emf estimation scheme under both no load as well as loaded condition. Fig 4.11 shows the Simulink model of Back emf MRAS scheme.
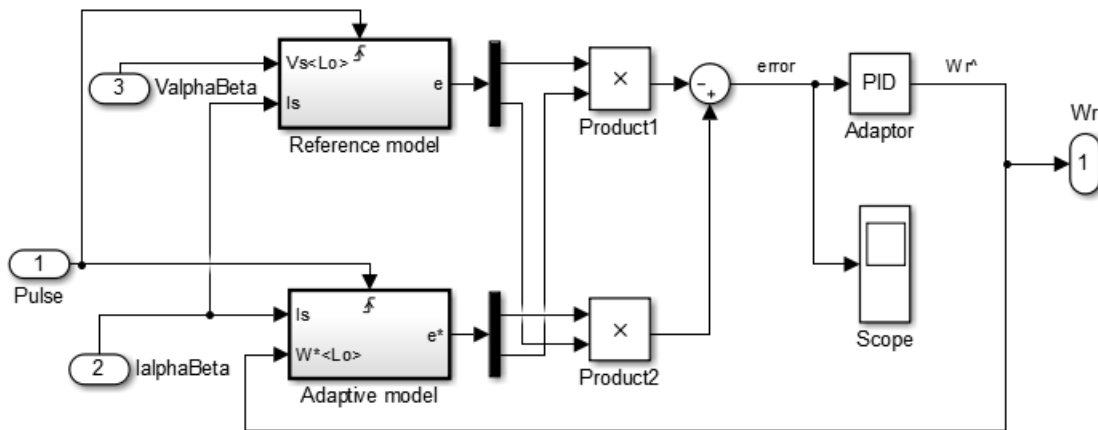

Fig.4.11 The Simulink model of Back emf MRAS scheme

Fig 4.12 illustrates the results with back emf based estimation scheme under no load condition. Ref. speed actual speed and estimated speed are presented in first segment with a step change in Ref. speed from 0 rpm to 100 rpm at 1 sec, 100 rpm to 0 rpm at 3 sec, 0 rpm to -100 rpm at 5 sec and -100 rpm to 0 rpm at 7 sec. At steady state, the estimated rotor speed reaches the actual speed. Load torque and generated torque are shown in second segment. Adaption signal which is the difference between the back emfs computed by the reference model and the adaptive model is shown in third segment.

To observe estimator's response under loaded condition, step change in load torque is applied by maintaining Reference speed at a constant value and step change in Reference speed is initiated while the load torque is constant. Fig 4.13 represents the system's response under loaded condition. Ref. speed, actual measured rotor speed and the estimated rotor speed are presented in first segment. Load torque and generated torque are shown in second segment. Adaption signal which is the difference between the back emfs computed by the reference model and the adaptive model is shown in third segment.
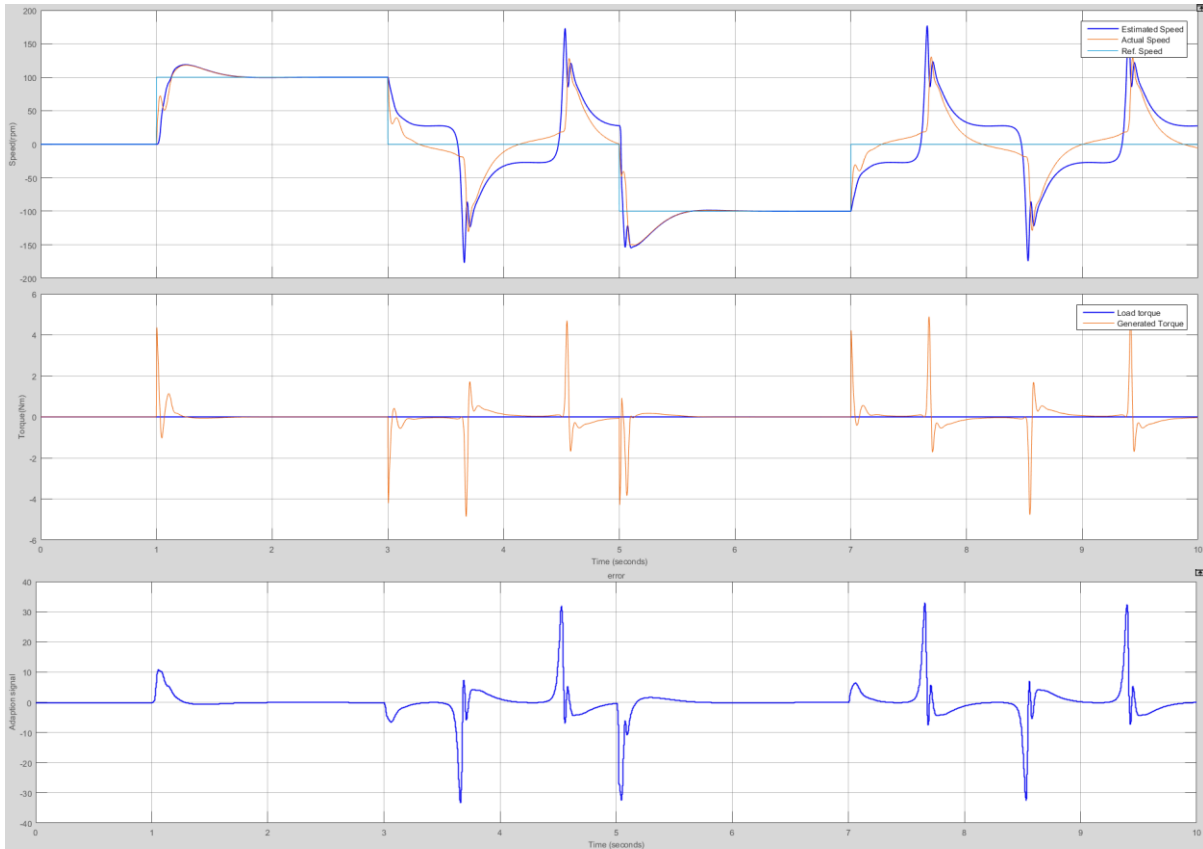
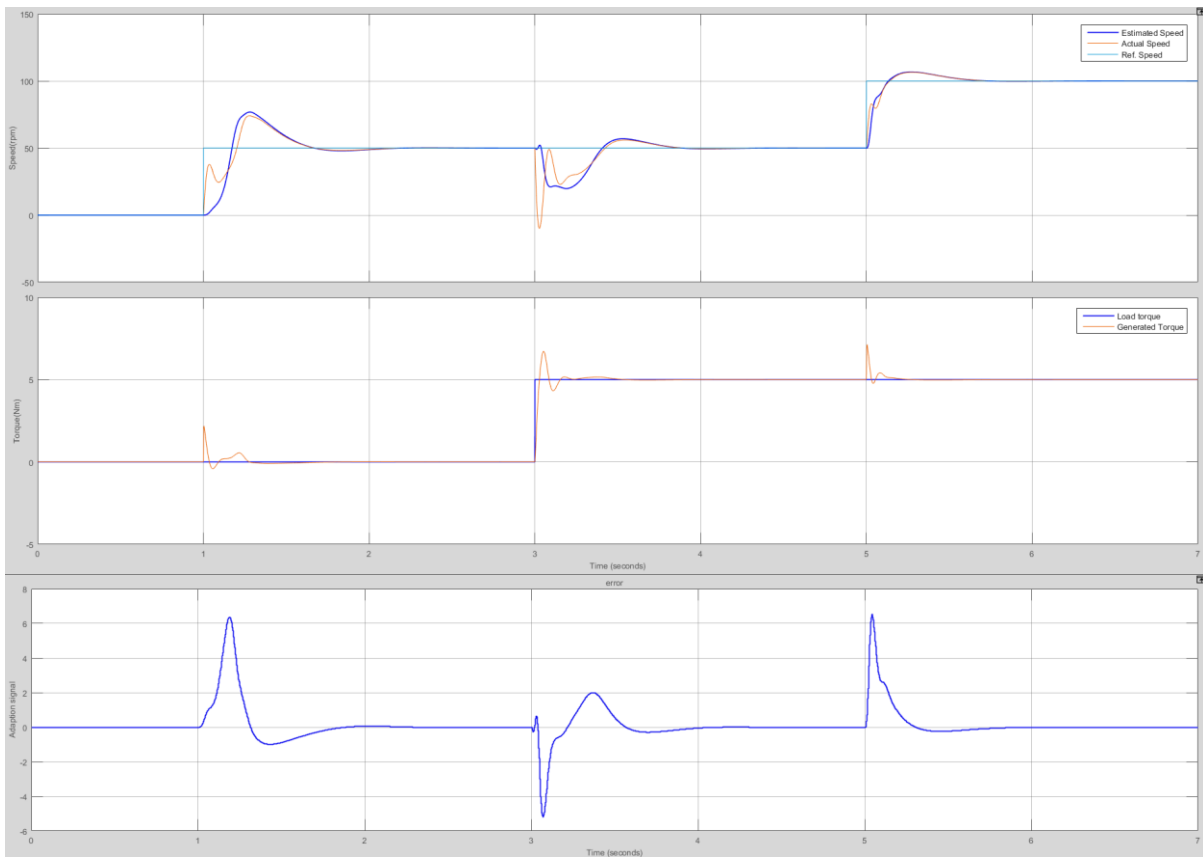Fig.4.12 Back emf MRAS Estimator Performance under No Load condition

Fig.4.13 Back emf MRAS Estimator Performance under Load condition

4.6.3 Reactive power MRAS scheme

Simulations are performed under no load condition as well as loaded condition with the reactive power based MRAS estimator. Fig 4.14 shows the Simulink model of Reactive power MRAS scheme.
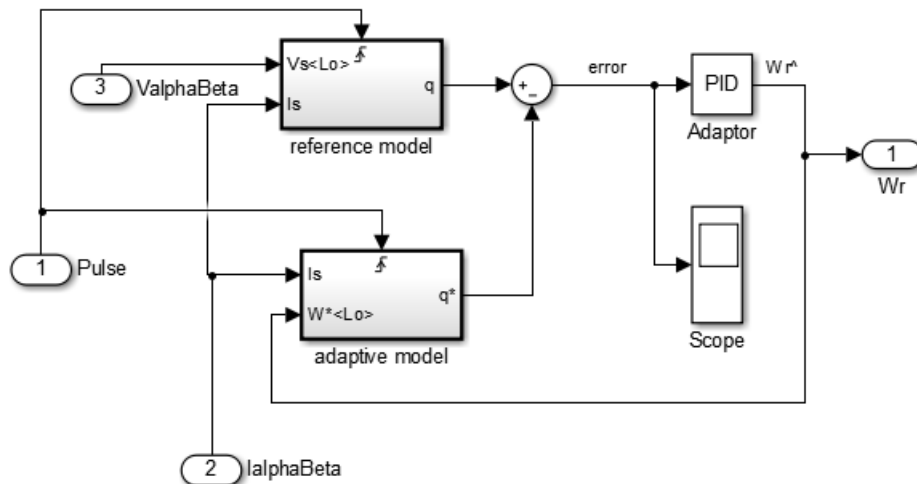
Fig.4.14 The Simulink model of Reactive power MRAS scheme

The dynamic performance of the estimator can be observed for sudden change in speed by initiating step change in Ref. speed at 1 sec, 3 sec, 5 sec and 7 sec and the results are presented in Fig 4.15. Ref. speed, actual measured rotor speed and the estimated rotor speed are presented in first segment. At steady state, the estimated rotor speed reaches the actual speed. Load torque and generated torque are shown in second segment. Adaption signal which is the difference between the reactive powers computed by the reference model and the adaptive model is shown in third segment.

To observe estimator's response under loaded condition, step change in load torque is applied at 3 sec by maintaining Reference speed at 50 rpm and step change in Reference speed is initiated at 5 sec while the load torque is at 5 Nm. Fig 4.16 represents the system's response under loaded condition. Ref. speed, actual measured rotor speed and the estimated rotor speed are presented in first segment. Load torque and generated torque are shown in second segment. Adaption signal which is the difference between the reactive powers computed by the reference model and the adaptive model is shown in third segment.

Fig.4.15 Reactive power MRAS Estimator Performance under No Load condition

Fig.4.16 Reactive power MRAS Estimator Performance under Load condition

4.6.4 Effect of parameter variation
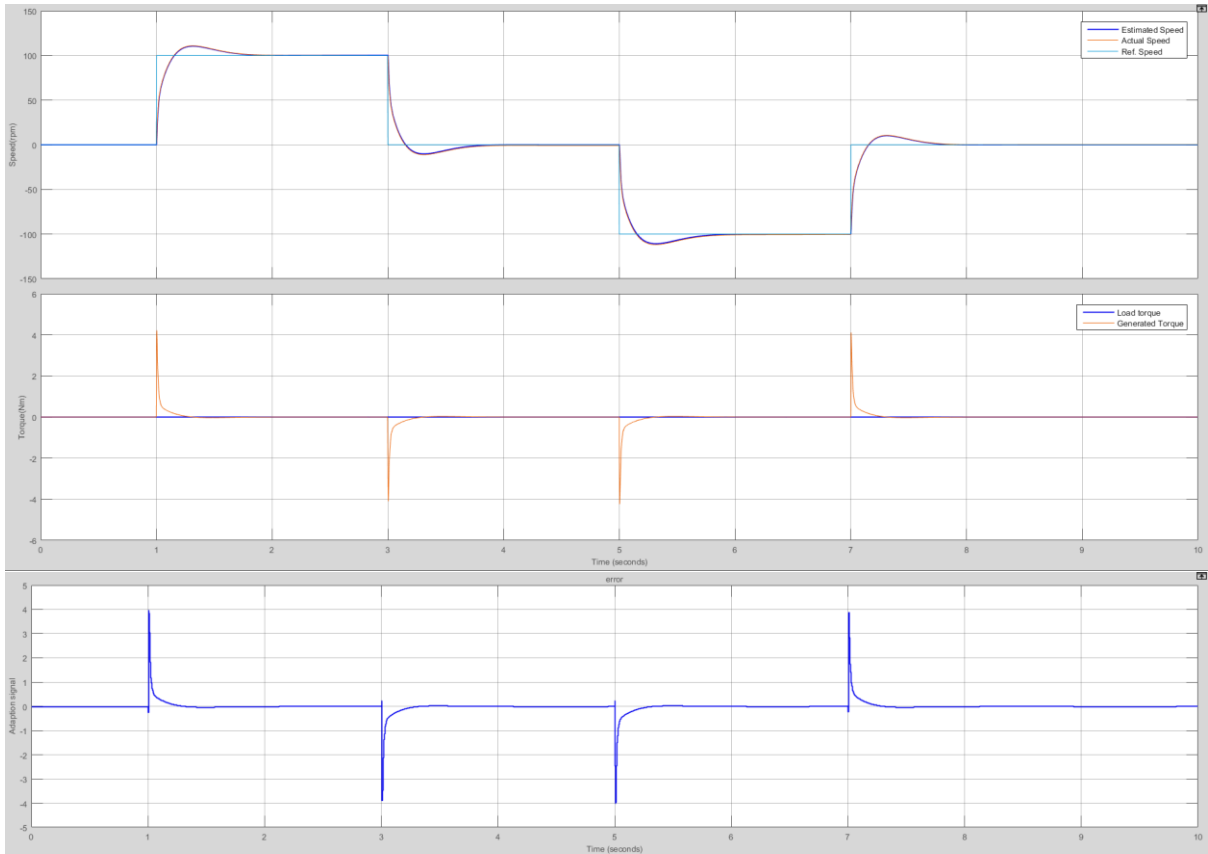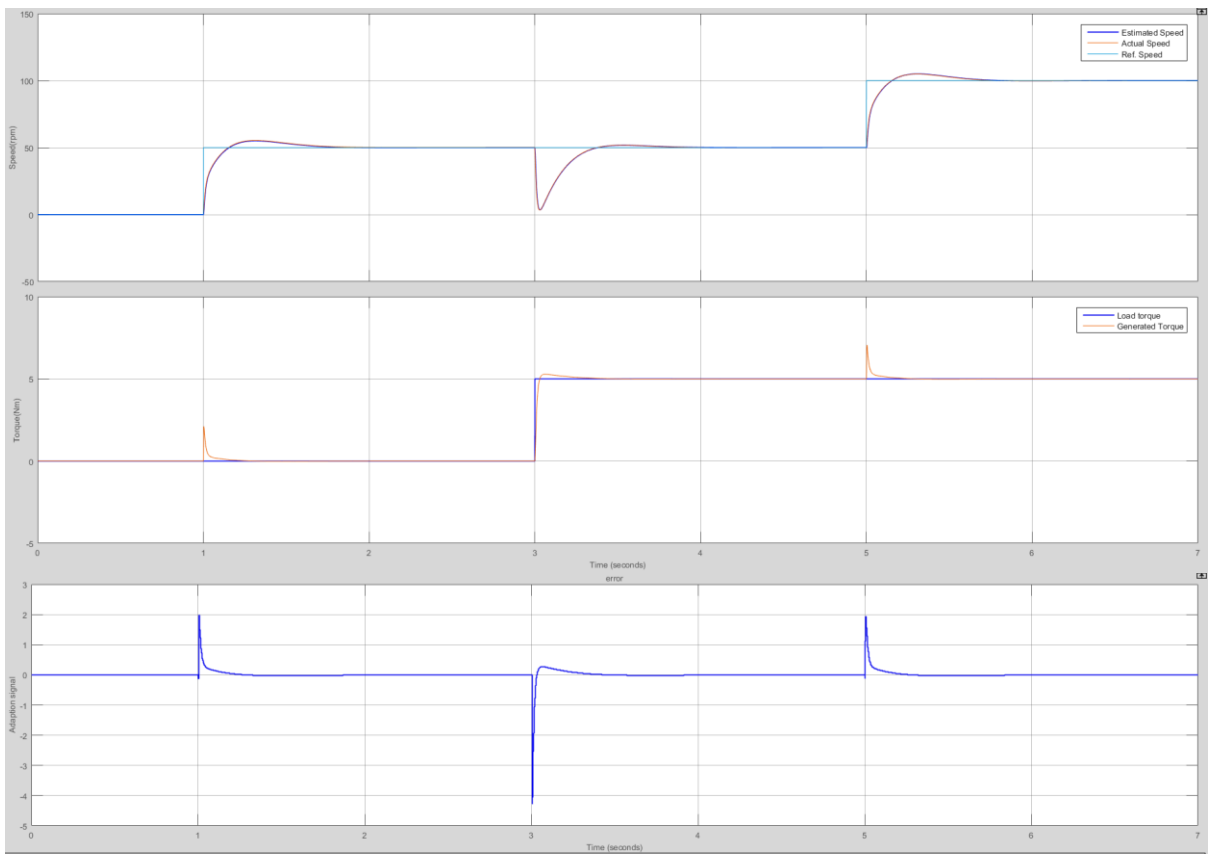
The effect of variation of stator resistance and mutual inductance is presented to observe the system's performance with the above speed estimators. The effect of variation of rotor resistance, rotor time constant and leakage inductance is negligible. The change of parameters is applied for the entire control algorithm by maintaining the original parameters in Induction machine model so that the effect can be observed if there is mismatch of the parameters used for speed control of IM. For comparison purpose the effect of change is presented for the model with sensor i.e. Indirect Vector Control model described in Chapter 3 where the speed from the Induction machine is used as feedback for speed control as well as rotor flux angle calculation.

4.6.4.1 Effect of 20% increase in stator resistance

When stator resistance is raised to 120% while keeping the remaining parameters unmodified, the results are as in Fig 4.17.

From Fig 4.17, it can be observed as Reactive power scheme is independent of stator resistance, there is no effect of the change in resistance. In Rotor flux scheme, at 50 rpm, estimator performance is good before as well as after applying load torque though having spikes while the speed obtained from IM model is having steady state error. At the step change in Ref. speed from 50 rpm to 100 rpm, both the speed from IM model and estimated speed are oscillating around the Ref. speed. In Back emf scheme, before applying load torque, estimator performance is good but after applying load torque, it is going unstable.
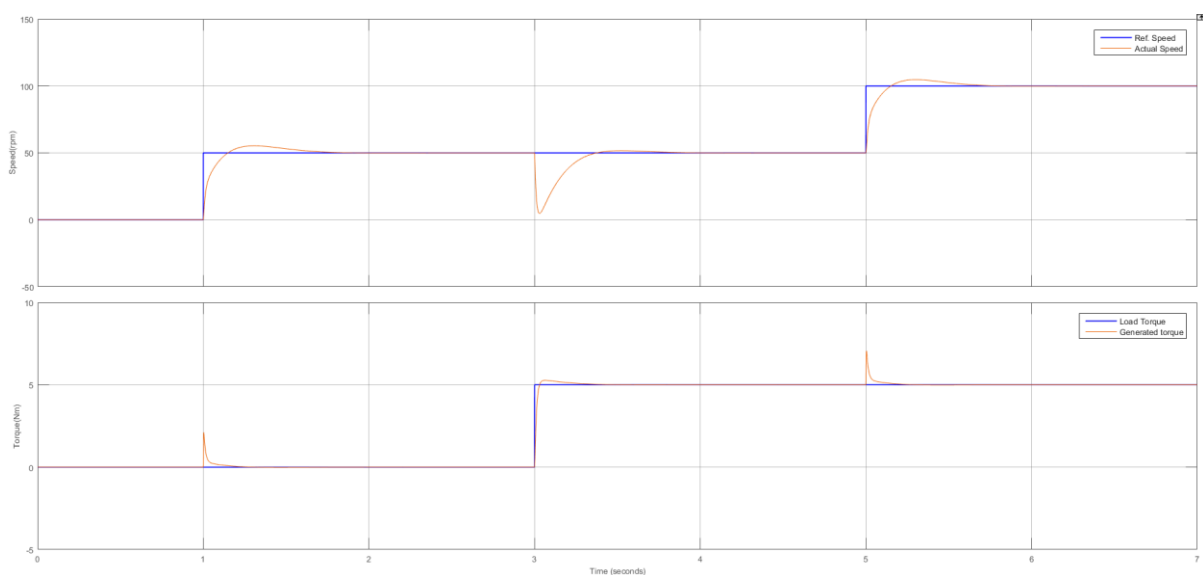
(a) With Sensor

(b) With Rotor flux MRAS

(c) With Back emf MRAS

(d) With Reactive power MRAS
Fig.4.17 The performance of the estimators for 20% increase in stator resistance

4.6.4.2 Effect of 20% decrease in stator resistance
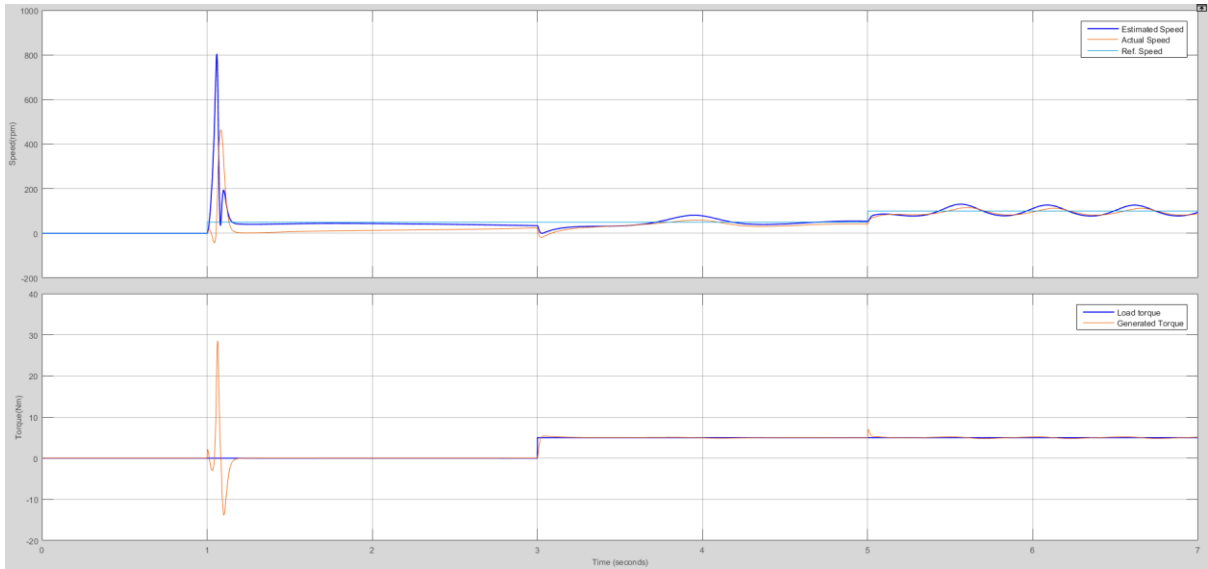
When stator resistance has been decreased to 80% while keeping the remaining parameters unmodified, the results are as in Fig 4.18.
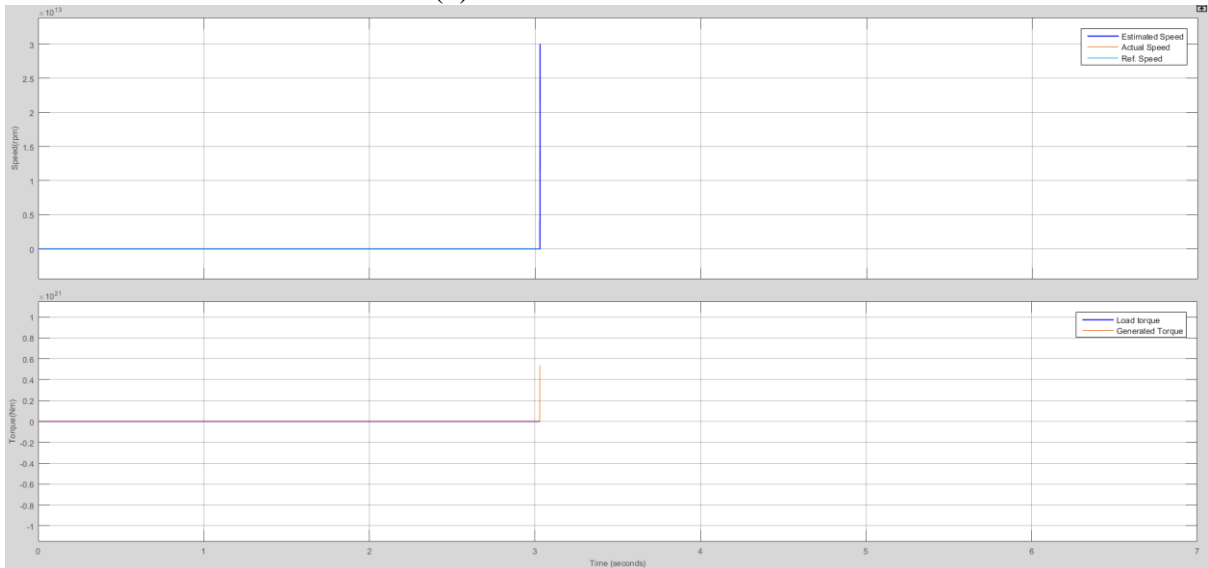
From Fig 4.18, it can be observed as Reactive power scheme is independent of stator resistance, there is no effect of the change in resistance. In Rotor flux scheme, estimated speed and the speed obtained from IM model are having oscillatory nature as soon as there is a step change in Ref. speed from 0 rpm to 50 rpm even before applying load torque. In Back emf scheme, estimator performance is satisfactory before as well as after applying load torque while the speed from IM model is having steady state error.

4.6.4.3 Effect of 20% increase in mutual inductance

When mutual inductance has been increased to 120% while keeping the remaining parameters unmodified, the results are as in Fig 4.19.

From Fig 4.19, it can be noticed that the Rotor flux estimator performance is very good with step change in Ref. speed under both no load condition as well as loaded condition, step change in load torque and the speed obtained from IM model is having steady state error under loaded condition. In Back emf scheme, the estimator performance is good though it is taking more time to reach the reference speed and the speed from IM model is having steady state error under loaded conditions. In Reactive power scheme, the estimator performance is satisfactory though it is taking more time to reach the reference speed and the speed from IM model is having steady state error.

4.6.4.4 Effect of 20% decrease in mutual inductance

When mutual inductance has been decreased to 80% while keeping the remaining parameters unmodified, the results are as in Fig 4.20.

From Fig 4.20, it can be noticed that the performance of both the Rotor flux scheme and Back emf schemes are very good. But the Reactive power MRAS estimator is going unstable even before applying load torque with 20% decrease in the mutual inductance.
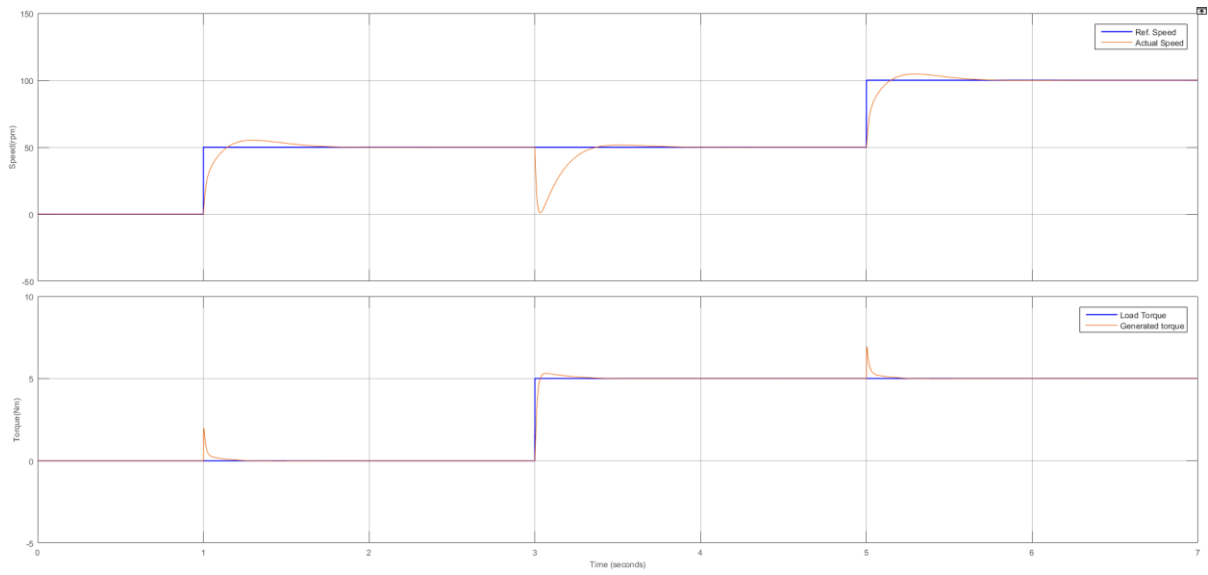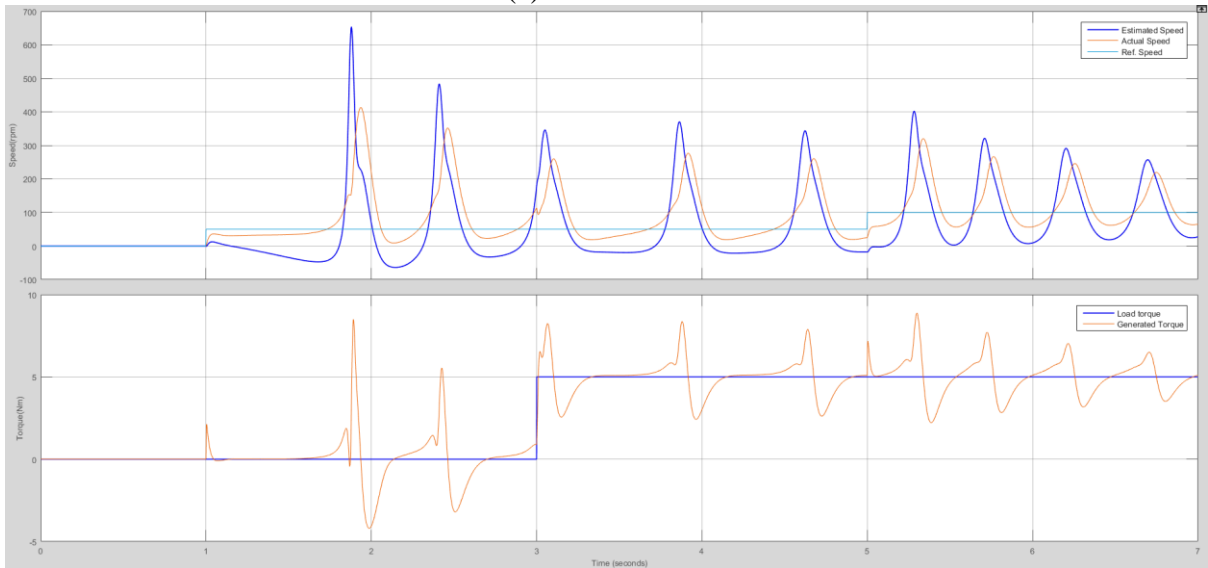
(a) With Sensor

(b) With Rotor flux MRAS
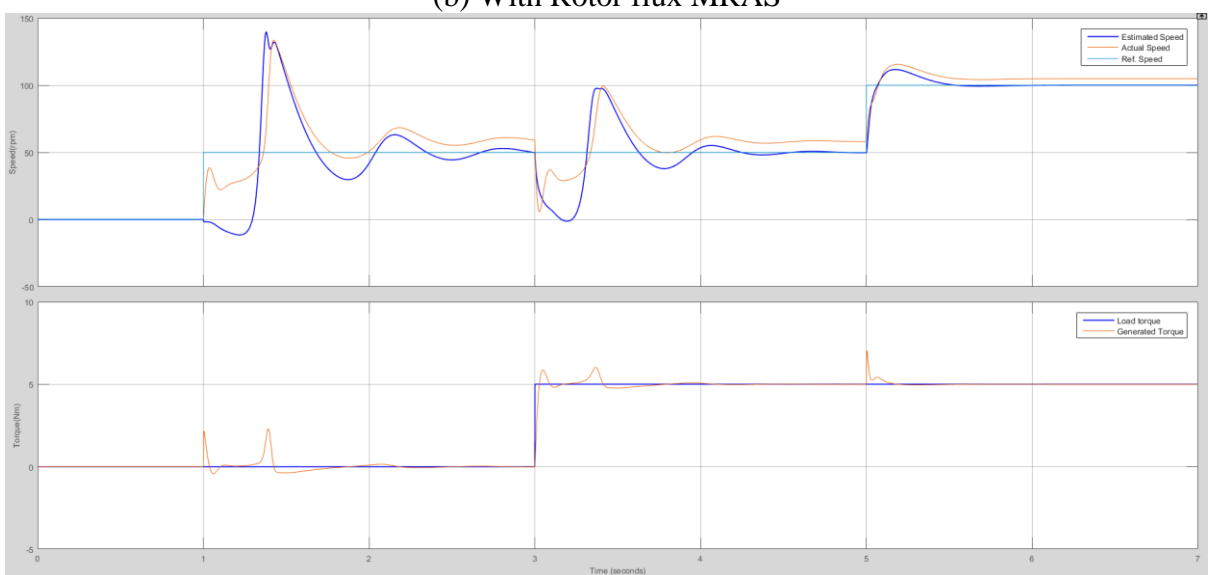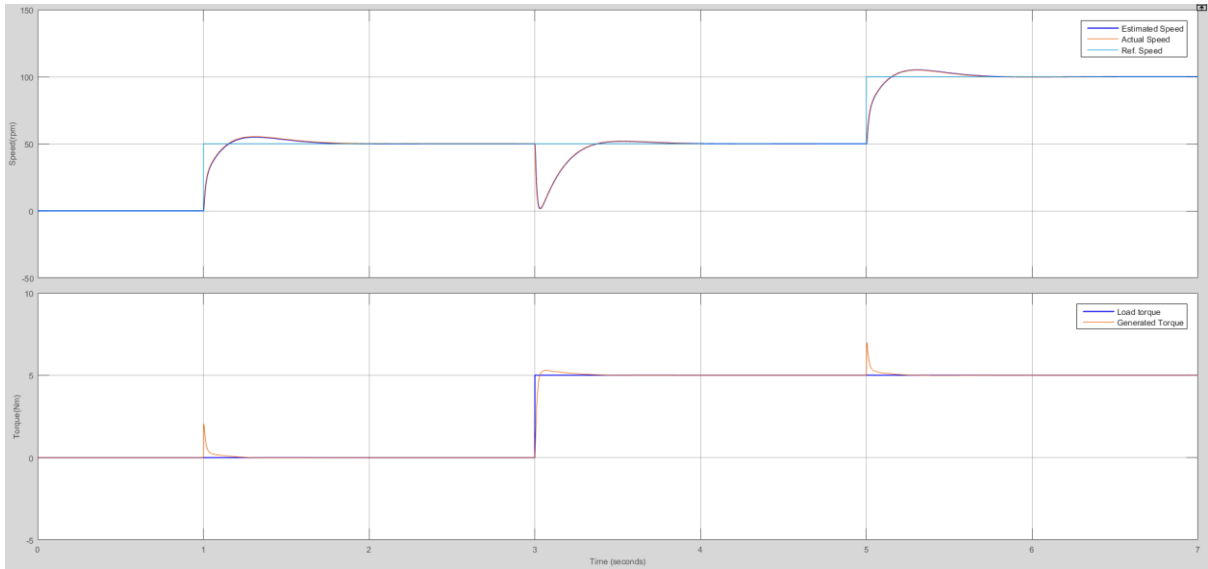
(c) With Back emf MRAS

(d) With Reactive power MRAS

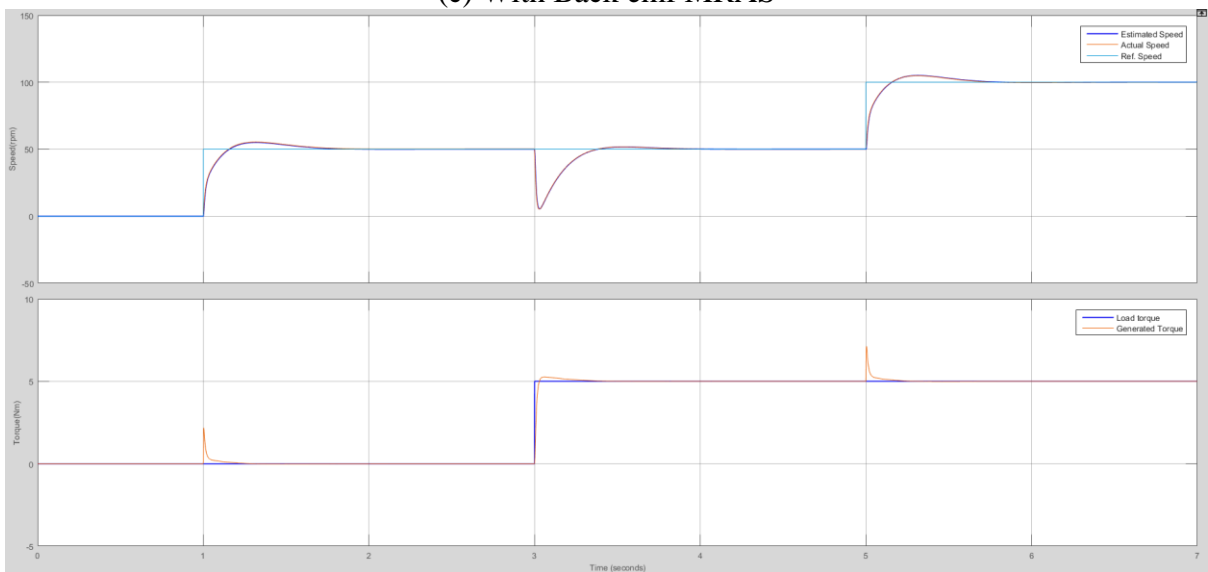Fig.4.18 The performance of the estimators for 20% decrease in stator resistance
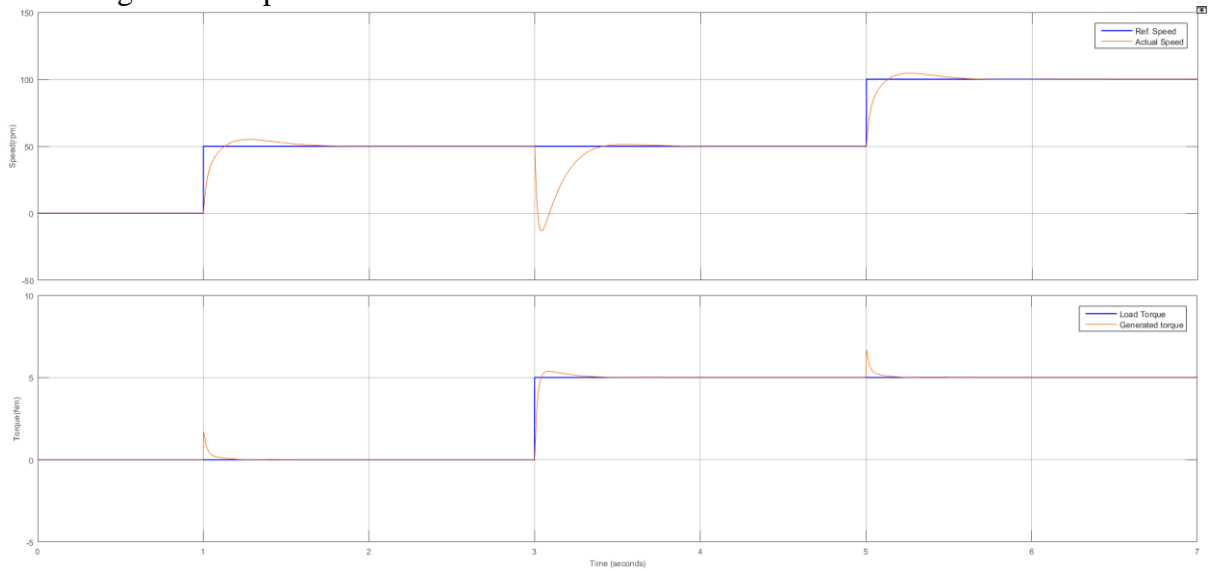
(a) With Sensor
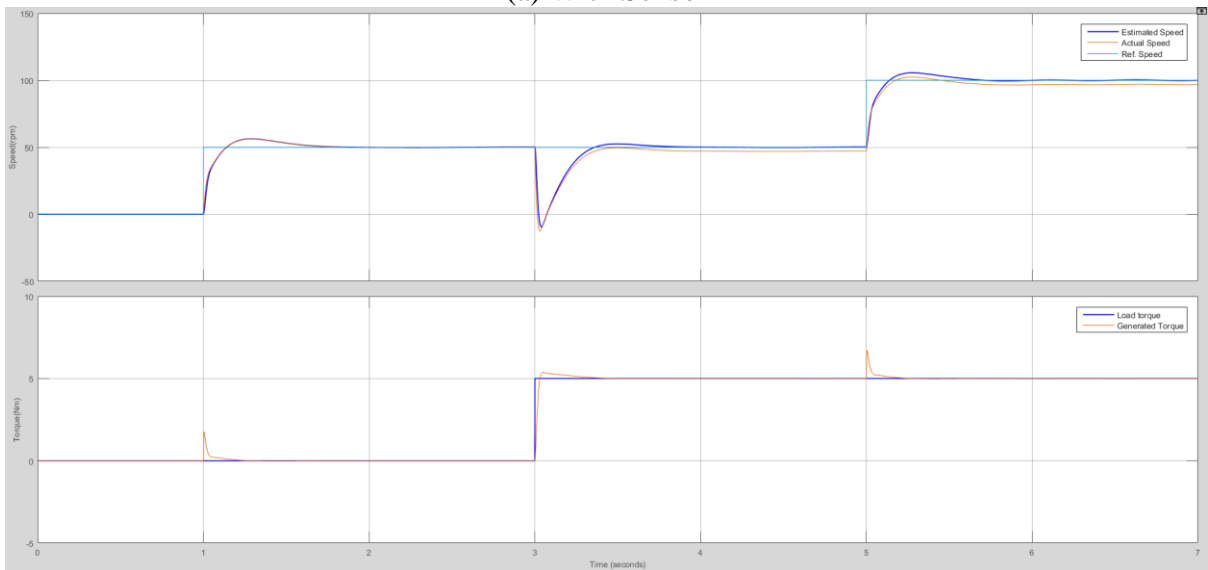
(b) With Rotor flux MRAS
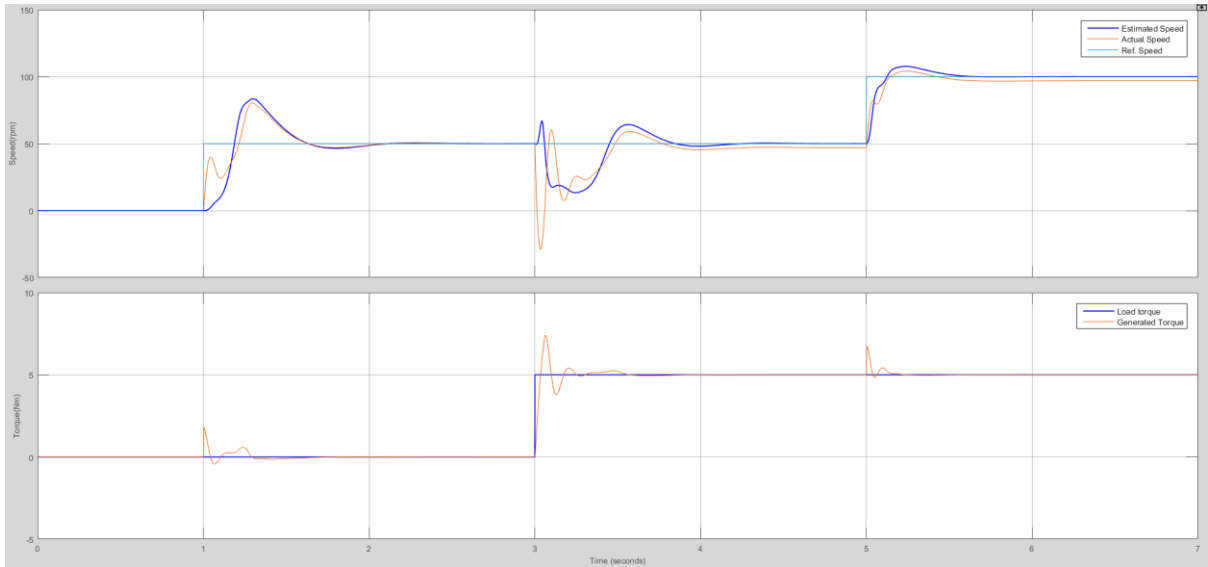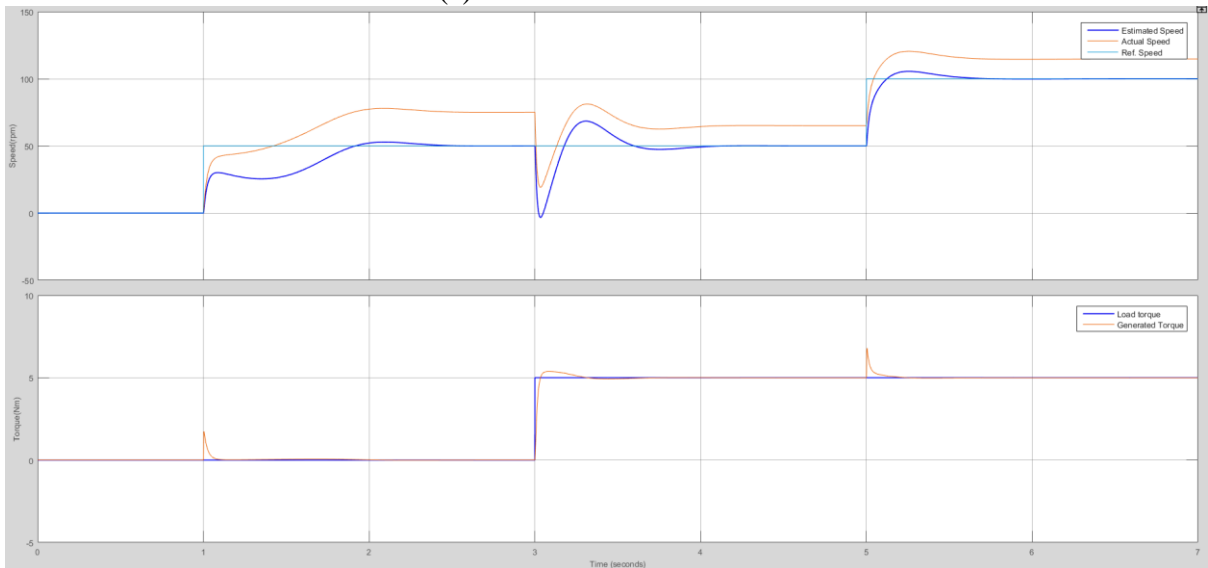
(c) With Back emf MRAS

(d) With Reactive power MRAS

Fig.4.19 The performance of the estimators for 20% increase in mutual inductance

(a) With Sensor

44
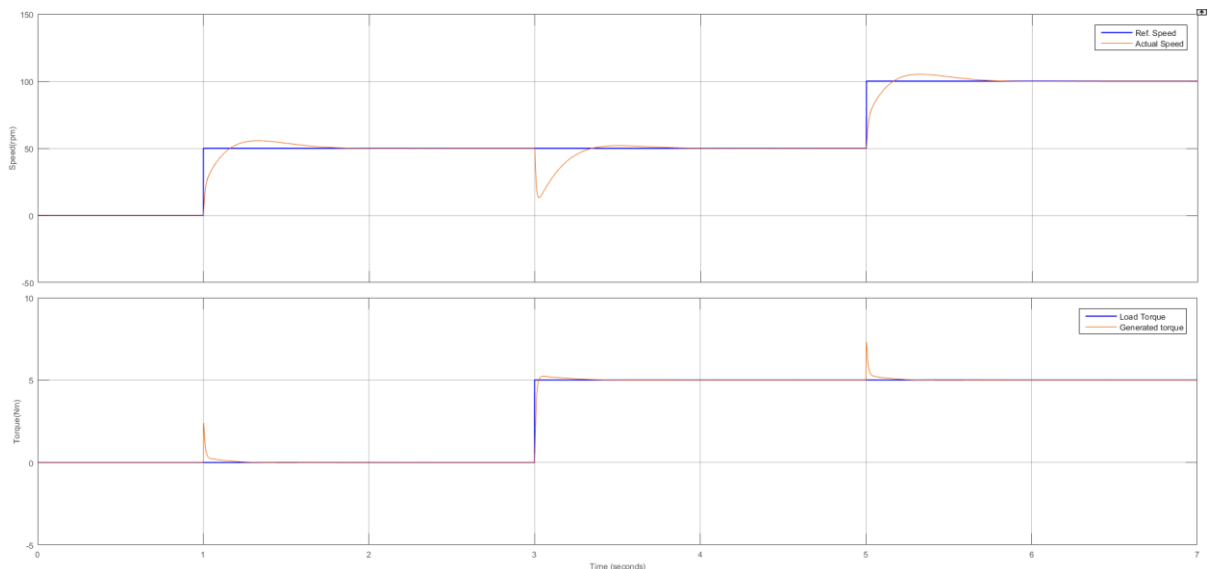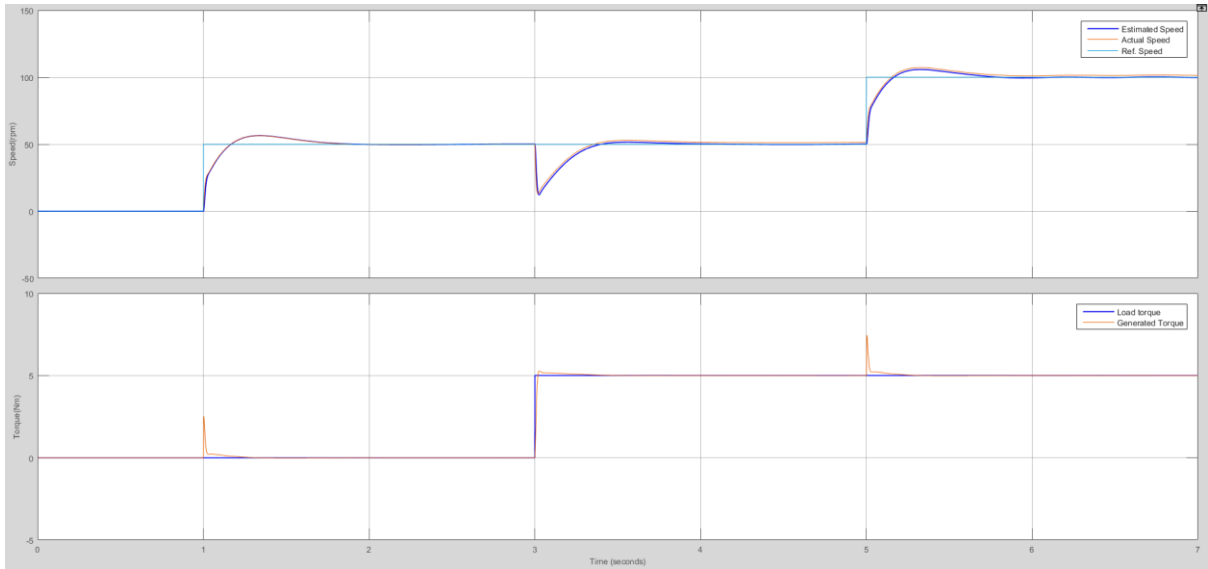
(b) With Rotor flux MRAS
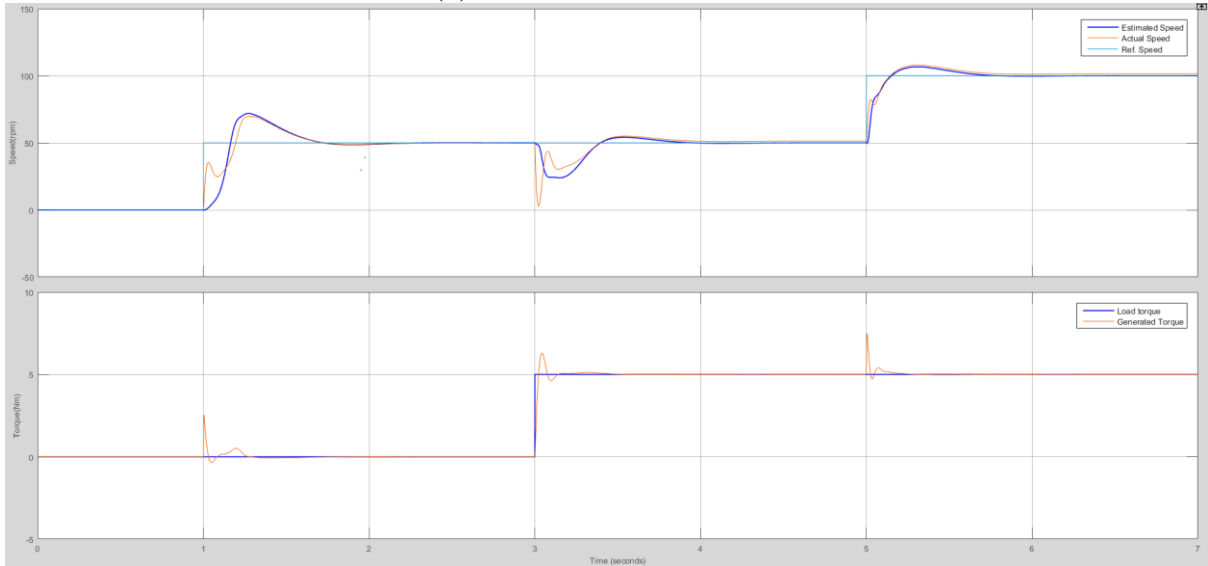
(c) With Back emf MRAS
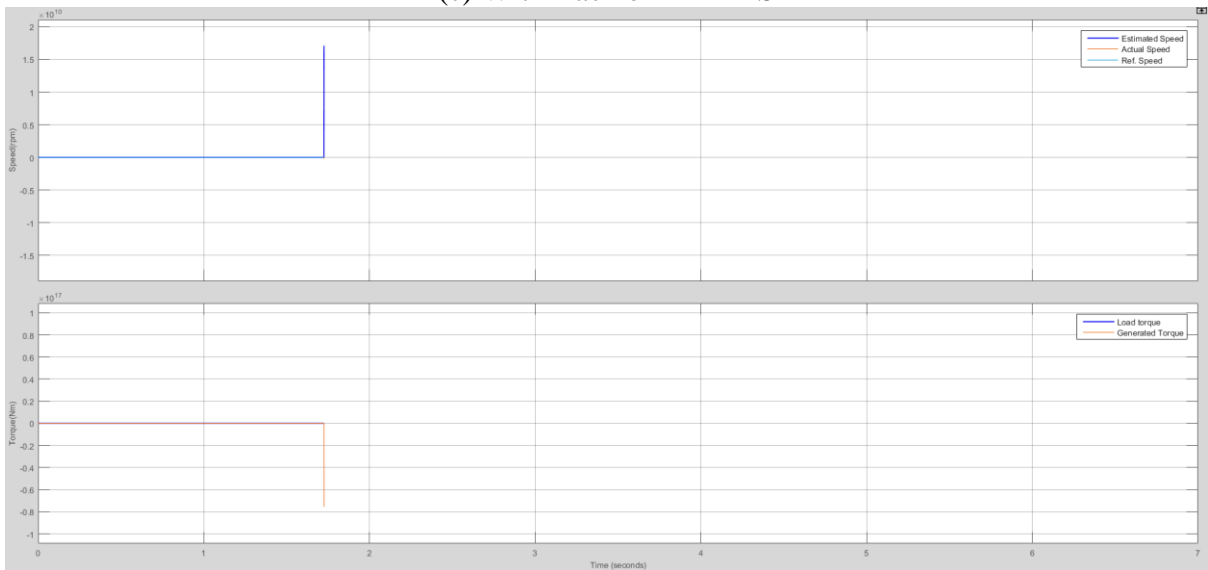
(d) With Reactive power MRAS

Fig.4.20 The performance of the estimators for 20% decrease in mutual inductance

45

4.7 Summary

In this chapter, indirect vector controlled induction motor is simulated by using MRAS speed estimation methods based on the rotor flux, back emf and reactive power. The stability of the system is guaranteed with Popov's inequality criterion for hyper stability of nonlinear time varying system.

Both the Steady state response and Dynamic response of the system with the above Estimation techniques are observed. The system is found to be stable with all the schemes for a sudden change in Ref. speed as well as with the sudden application of load torque.

Rotor flux MRAS estimator and Back emf MRAS estimator are not independent of stator resistance. The effect of variation of stator resistance on both the estimators has been observed. With 20% increase in stator resistance, Back emf based MRAS system becomes unstable. In Rotor flux based MRAS system, with 20% decrease in stator resistance, oscillations are observed in estimated rotor speed and that is responsible for torque oscillations which cannot be tolerable.

Instantaneous Reactive power MRAS estimator is sensitive to the mutual inductance. With 20% decrease in mutual inductance, system becomes unstable. Therefore it is necessary to know the correct mutual inductance value.

It is obvious that stator resistance varies with the temperature especially in the case of heavy duty machines. In Rotor flux MRAS estimator and Back emf MRAS estimator, Resistance variation will cause inaccuracy in estimation. One more limitation of the Rotor flux MRAS technique is the requirement of pure integration in its Voltage model which causes the drift in calculation of rotor flux. Additionally setting initial conditions for the integrator is also difficult. Therefore, the Rotor flux MRAS estimator is not advisable to use practically. Back emf based estimator is very sensitive at low speed operation as the back emf generated is very low under low frequencies. Therefore Back emf based scheme is not recommended for low speed operation. On the other hand the reactive power MRAS estimator is completely independent of stator resistance and doesn't require open loop integration and its performance is satisfactory under low speed operation. Hence the performance of instantaneous reactive power MRAS estimator can be assured in practical system.

5. Hardware

5.1 Overview

An integrated DSP (Pentium Processor) system is used for implementing the reactive power based MRAS scheme. Fig 5.1 represents the complete experimental setup. It needs few number of external interface peripherals. Two terminal line to line voltages and currents of the induction motor are measured by using voltage sensor and current sensor and has been interfaced to the A/D converters built in the processor. A speed sensor to measure the actual rotor speed of the induction motor is interfaced to the encoder interface built in the processor.
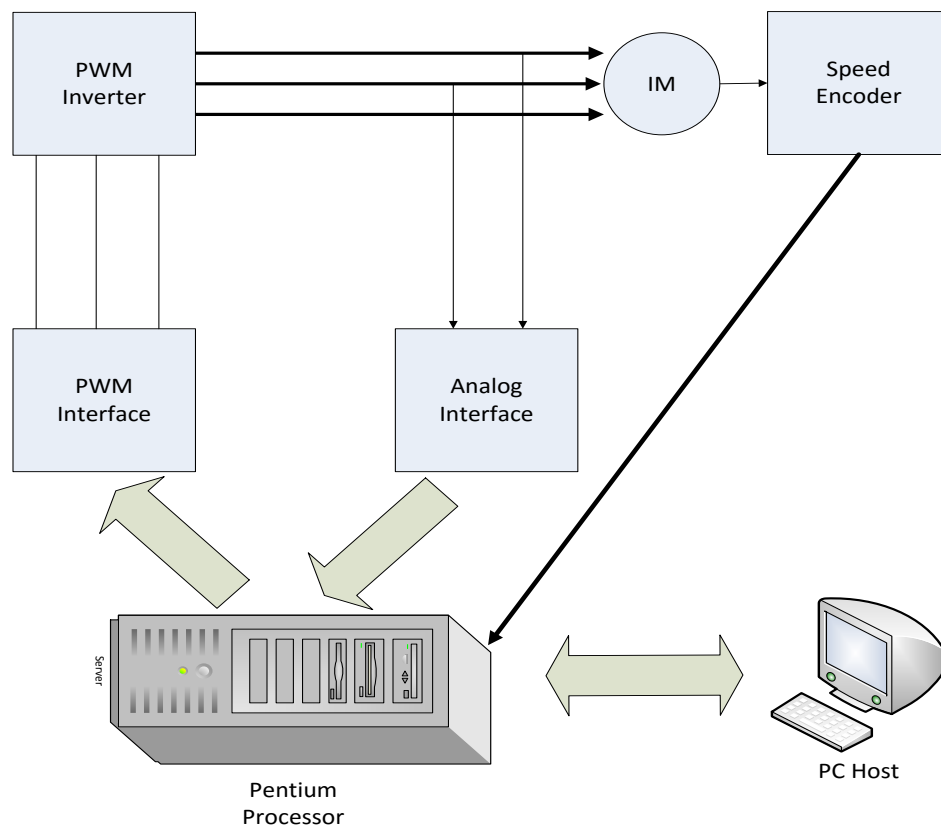
Fig.5.1 Experimental setup

Pentium processor acts as the Kernel while the Linux operating system in the PC host is used for programming in 'C' language. The program is given in Appendix. The parameters of the Induction Motor are estimated at rated current. To obtain more approximate parameters, several measurements have been taken and then average of the measurements is computed. The

calculated motor parameters and the functions used for the estimation are mentioned in the program.

5.2 Results & Discussion

In this chapter, implementation of Reactive power based MRAS scheme on an experimental test bench is done by using an integrated DSP based system. Due to equipment limitation, the experiments are done only under No-load conditions. The results are shown in Fig 5.2.

Fig 5.2 shows the performance of the Reactive power based MRAS scheme under different conditions. Reference speed, actual speed, estimated speed and q-axis currents are presented for each case. Estimated speed is used as feedback to control the speed as well as to calculate the angle of rotor flux. Actual speed is presented to show the noise in the cable. The steady state performance and dynamic performance of the system is satisfactory with the correct estimation of parameters except at very low speeds. The estimator performance is good till 20 rad/sec and if the reference speed is less than 20 rad/sec, estimated speed is having some steady state error.

To observe the performance of the estimator under the parameter variations, experiments are done with the change in stator resistance, rotor resistance, rotor time constant, leakage inductance and mutual inductance. The effect of the parameter change is negligible for all these parameter changes except with the decrease in mutual inductance. When we use 90% of the actual mutual inductance value in the control algorithm, the system becomes unstable as shown in (d) section of Fig 5.2.
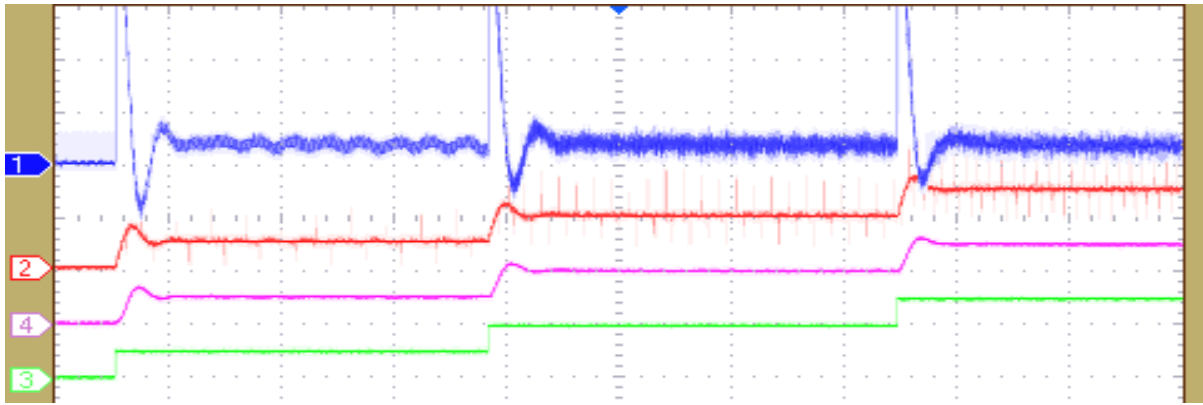
(a) With step increase of reference speed
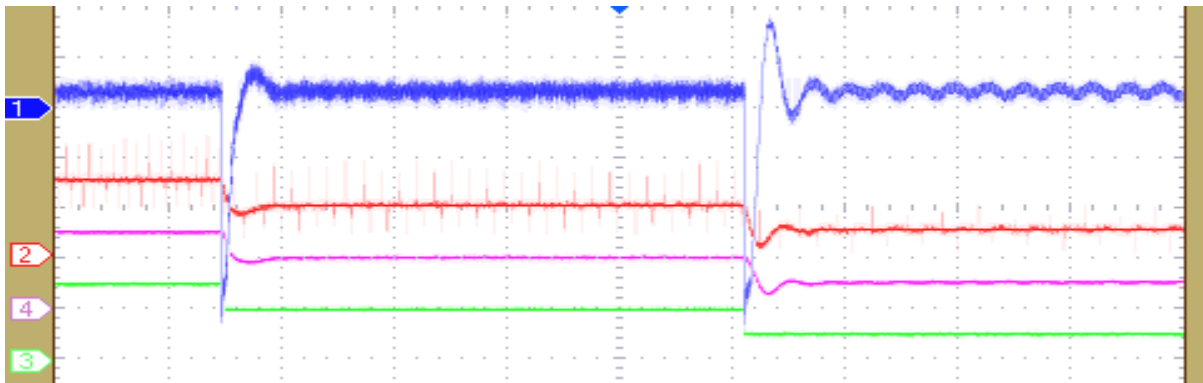
(b) With step decrease of reference speed
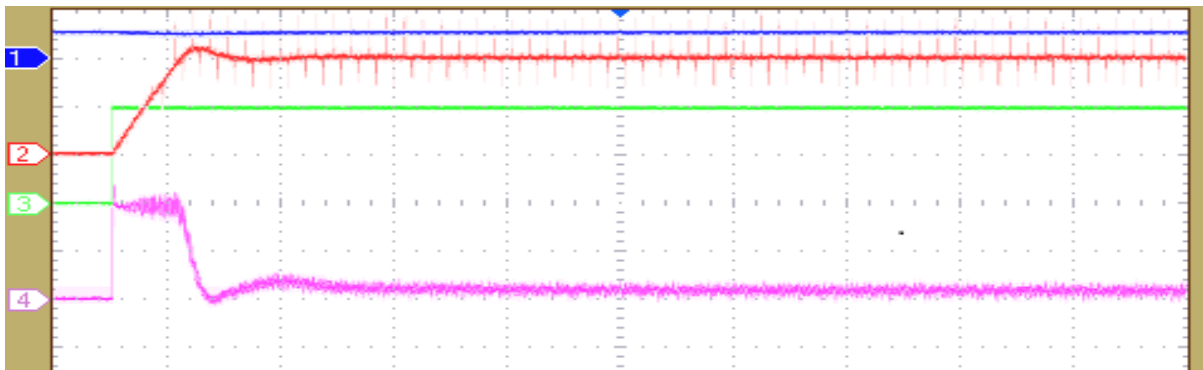
(c) With large step change of reference speed
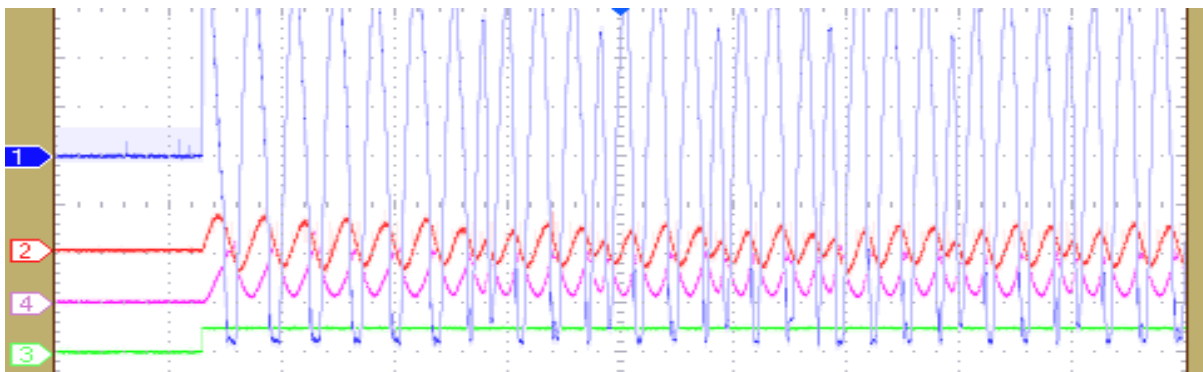
(d) With 10% decrease in mutual inductance

Fig.5.2 Performance of Reactive power MRAS scheme

5.3 Summary

The practical results presented in this chapter show that very good performance can be achieved from a sensor less vector control drive provided that the machine parameters are accurately known. The dynamic performance of such sensor less system has been found to be comparable to sensored implementations, although not outstanding.

The practical results shown in this chapter are consistent with the predicted theoretical results shown in Chapter 4 in terms of speed accuracy, system stability and parameter sensitivity. In view of these theoretical results, the practical results shown in this chapter also confirm the necessity of accurate estimation of mutual inductance in order to obtain good performance from the sensor less drive using the Reactive power based MRAS scheme.

6. Conclusion

❖ Induction motor is mathematically modelled in stator reference frame and Simulation results are presented.

❖ The indirect vector controlled induction motor is simulated using PI controller and the responses are studied using both load torque and speed variation.

❖ To improve the reliability of system, sensor-less speed control is studied using rotor flux, back emf and instantaneous reactive power based MRAS techniques. Simulation of these models are implemented under both no-load as well as loaded conditions.

❖ The effect of change in the motor parameters is presented to observe the performance of the IM with the speed estimators. And reactive power based MRAS scheme is found to be suitable for practical implementation at low speed operation.

❖ By using an integrated DSP based system, reactive power based MRAS scheme is implemented on an experimental test bench and observed that the performance is comparable to sensored drive operation.

APPENDIX

Main Header File (.h):

```c
// global physical quantities
extern float Ualpha, Ubeta, Ud, Uq, id, iq, omega_MRAS_q,
omega_MRAS_q_filter;

//field oriented control algorithm
void FOC(float tar_id, float tar_iq, float phi);

//Space Vector Modulation
void SVM(float ualpha, float ubeta, int* satflag);

//speed estimator MRAS : reactive power based
void speed_estimator_MRAS_q(void);

// rotor flux observer
void rotor_flux_observer(float *psi_r_alpha, float *psi_r_beta,
float ialpha, float ibeta, float omega, float Fs);

//-------------------------------------------------------------
//                        PI-Controller

// flux_controller (PI) with Anti-Windup
void flux_controller(float target_flux, float flux, float *tar_id);

// speed control (PI) with Anti-Windup
void speed_controller(float target_omega, float omega, float
*tar_iq);

//-------------------------------------------------------------
//                        Call this function

// speed control of induction machine
void control_system(void);

// Estimate Stator Resistance
void estimate_Rs(void);

// Estimate Stator leakage inductance
void estimate_L_ls(void);

// Estimate flux psi_r^d
void flux_psi_r_d(void);

// Rotor time constant
void rotor_time_constant(void);
```

C Source File (.c):

```c
#include <rtai_math.h>
#include <rtai_sched.h>

#include "control.h"
#include "pentium.h"
#include "toolbox.h"

//-------------------------------------------------------------
//                          To Edit
//-------------------------------------------------------------
//                      Motor parameters

//Stator resistance
#define R_s 3.2

//Rotor resistance
#define R_r 1.485

// Stator inductance
#define L_s 0.352

// Rotor inductance
#define L_r 0.352

//timeconstant rotor cage
#define tau_r 0.237

//leackage inductance
#define L_ls 0.0322

//mutual inductance
#define M 0.32

// sigma of ASM
#define sigma 0.092

// Rotor Inertia
#define J 0.05

//-------------------------------------------------------------

// current control gains
#define GP_FOC 0.07
#define GI_FOC 0.5

// flux control gains
#define GP_flux 0.1
#define GI_flux 20

//rotor speed control
#define GP_omega 0.1
#define GI_omega 0.01
```

```c
//speed estimator MRAS_q gains
#define GP_MRAS_q 0.1
#define GI_MRAS_q 0.01


//-------------------------------------------------------------
//                      Limit for Anti-Windup

//current limit
#define imax 5.0

// lower limit flux
#define i_flux_min 0.002

// nominal flux
#define psi_r_d 1.1

//flux limit
#define Psi_max 1.5

// nominal mechanical angular velocity
#define omega_M_nenn 297.4

// maximal mechanical angular velocity
#define omega_max 500.0


//-------------------------------------------------------------
//                      global physical quantities

float Ualpha              = 0.0;
float Ubeta               = 0.0;
float Ud                  = 0.0;
float Uq                  = 0.0;
float id                  = 0.0;
float iq                  = 0.0;
float omega_MRAS_q        = 0.0;
float omega_MRAS_q_filter = 0.0;
//-------------------------------------------------------------

//fiel oriented control algorithm

void FOC(float tar_id, float tar_iq, float theta)
{
    static float Vi, Vu;
    static float integral_d = 0.0;
    static float integral_q = 0.0;
    static float costheta, sintheta;
    static int satflag = 0;
    static int over_current = 0;
    static float pulse = 0.0;
    static float toggle;
    static float test;

    //over current check
    if(ialpha*ialpha + ibeta*ibeta > 7.0*7.0) PWM_disable();
```

```c
//limit current
Vi = (tar_id*tar_id+tar_iq*tar_iq)/(imax*imax);

if(Vi>1.0)
{
    Vi = sqrt(Vi);
    tar_id /= Vi;
    tar_iq /= Vi;
}

//calculate cos and sin only once
costheta = cos(theta);
sintheta = sin(theta);

//transform actual currents to rotating fixed frame
id =  ialpha*costheta + ibeta*sintheta;
iq = -ialpha*sintheta + ibeta*costheta;

//calculate voltages in rotating fixed frame
Ud = GP_FOC * (tar_id - id);      //P-part
Uq = GP_FOC * (tar_iq - iq);

Ud += integral_d;             //Sum P+I
Uq += integral_q;

//voltage limit 0.866 circle and anti windup
Vu = (Ud*Ud + Uq*Uq)/(Udc*Udc);

if(Vu>1.0)
{
    Ud /= Vu;
    Uq /= Vu;
    integral_d = 0;
    integral_q = 0;
}
else
{
    //Integration
    integral_d += GP_FOC*GP_FOC*GI_FOC*(tar_id - id);
    integral_q += GP_FOC*GP_FOC*GI_FOC*(tar_iq - iq);

    // upper limit integral_d
    if(integral_d> +1.0)
        integral_d= +1.0;

    // lower limit integral_d
    if(integral_d< -1.0)
        integral_d= -1.0;
    // upper limit integral_q
    if(integral_q> +1.0)
        integral_q= +1.0;
    // lower limit integral_q
    if(integral_q< -1.0)
        integral_q= -1.0;

}
```

```c
        //transform voltages to stator fixed frame
        Ualpha = Ud*costheta - Uq*sintheta;
        Ubeta  = Ud*sintheta + Uq*costheta;

        //set PWM
        SVM(Ualpha, Ubeta, &satflag);
}


//Space Vector Modulation

void SVM(float ualpha, float ubeta, int* satflag)
{
        static float pr[3], pw[3], sumpw, satfactor;
        static int   i, pph[3];
        static float uar, ubr, ucr;
        static float moda_avg;
        static int avg_counter = 1;

        //projection perpendicular to phases (a=0, b=1, c=2)
        pr[0] =                    +1181.25*ubeta; pph[0] = 0;
        pr[1] = -1023.00*ualpha - 590.63*ubeta; pph[1] = 1;
        pr[2] = +1023.00*ualpha - 590.63*ubeta; pph[2] = 2;

        //sort by magnitude (only necessary that maxval is the last)
        for(i=0;i<2;i++)
              if (abs(pr[pph[i]])>abs(pr[pph[i+1]]))
                    iswap(pph+i,pph+i+1);

        //assign pulsewidths
        i = pph[1] - pph[0]; //sign dependent decission
        if((i&1)^(i<0))
        {
              pw[pph[1]] = +pr[pph[0]];
              pw[pph[0]] = -pr[pph[1]];
        }
        else
        {
              pw[pph[1]] = -pr[pph[0]];
              pw[pph[0]] = +pr[pph[1]];
        }
        pw[pph[2]] = 0;

        //limitation to hexagon (overmodulation)
        sumpw = abs(pw[pph[0]] - pw[pph[1]]);
        satfactor = (sumpw>1023.0)? 1023.0/sumpw : 1.0;
        *satflag  = (sumpw>1023.0)? 1:0;

        if(satfactor<1.0)
              pw[pph[0]] *= satfactor; pw[pph[1]] *= satfactor;

        //PWM references
        if(pw[pph[0]]<= pw[pph[1]])
              iswap(pph, pph+1);
```

```c
        //neccessary order: positive pulsewidth first
        mod[pph[0]] = (int)(0.5*(1023.0-sumpw)); //standard modulation

        //flattop for more than 60% pulsewidth
        mod[pph[2]] = mod[pph[0]] + (int)(pw[pph[0]]);
        mod[pph[1]] = mod[pph[2]] - (int)(pw[pph[1]]);

        mod[0] = 1023 - mod[0];
        mod[1] = 1023 - mod[1];
        mod[2] = 1023 - mod[2];

        //commands to PWM card
        outw(( mod[0] & 0x03FF) | 0x4000, PWM_CARD);
        outw(( mod[1] & 0x03FF) | 0x8000, PWM_CARD);
        outw(( mod[2] & 0x03FF) | 0xC000, PWM_CARD);
}


//speed estimator : MRAS : reactive power based

void speed_estimator_MRAS_q(void)
{
        static float d_ialpha = 0.0;
        static float ialpha_prev = 0.0;
        static float d_ibeta = 0.0;
        static float ibeta_prev = 0.0;
        static float psi_alpha_r = 0.0;
        static float psi_beta_r = 0.0;
        static float MRAS_q = 0.0;
        static float MRAS_q_e = 0.0;
        static float integral_MRAS_q = 0.0;

        d_ialpha = (ialpha - ialpha_prev)*Fs;
        d_ibeta = (ibeta - ibeta_prev)*Fs;

        ialpha_prev = ialpha;
        ibeta_prev = ibeta;

        psi_alpha_r += ((M/tau_r)*ialpha - psi_alpha_r*(1/tau_r) -
psi_beta_r*omega_MRAS_q)/Fs ;

        psi_beta_r += ((M/tau_r)*ibeta - psi_beta_r*(1/tau_r) +
psi_alpha_r*omega_MRAS_q)/Fs;

        MRAS_q = 2.0/3.0*Udc*(ialpha*Ubeta - ibeta*Ualpha) -
sigma*L_s*(ialpha*d_ibeta - ibeta*d_ialpha);

        MRAS_q_e = (M/L_r)*((1/tau_r)*(psi_alpha_r*ibeta -
psi_beta_r*ialpha) + omega_MRAS_q*(ialpha*psi_alpha_r +
ibeta*psi_beta_r));

        omega_MRAS_q = GP_MRAS_q*(MRAS_q-MRAS_q_e) + integral_MRAS_q;

        if(omega_MRAS_q > omega_M_nenn)
        {
                omega_MRAS_q = omega_M_nenn;
```

```
                integral_MRAS_q = 0.0;
        }

        else if(omega_MRAS_q < 0.0)
        {
                omega_MRAS_q =  0.0;
                integral_MRAS_q = 0.0;
        }
        else
        {
                integral_MRAS_q += GI_MRAS_q*(MRAS_q-MRAS_q_e);

                if(integral_MRAS_q > omega_M_nenn)
                        integral_MRAS_q = omega_M_nenn;
                else if(integral_MRAS_q < 0.0)
                        integral_MRAS_q = 0.0;
        }
        omega_MRAS_q_filter += 0.005*(omega_MRAS_q -
omega_MRAS_q_filter);
}

//speed estimator : MRAS : rotor flux based

void speed_estimator_MRAS_psi(void)
{
        static float psi_alpha_r_p = 0.0;
        static float psi_beta_r_p = 0.0;
        static float psi_alpha_r_a = 0.0;
        static float psi_beta_r_a = 0.0;
        static float psi_alpha_r_e = 0.0;
        static float psi_beta_r_e = 0.0;
        static float flux_error = 0.0;
        static float integral_MRAS_psi = 0.0;

        psi_alpha_r_p += (L_r/M)*(Ualpha*(2.0/3.0)*Udc -
R_s*ialpha)/Fs;

        psi_beta_r_p  += (L_r/M)*(Ubeta*(2.0/3.0)*Udc - R_s*ibeta)/Fs;

        psi_alpha_r_a = (L_r/M)*L_s*sigma*ialpha + psi_alpha_r_p;
        psi_beta_r_a  = (L_r/M)*L_s*sigma*ibeta + psi_beta_r_p;

        psi_alpha_r_e += ((M/tau_r)*ialpha - psi_alpha_r_e*(1/tau_r) -
psi_beta_r_e*omega_MRAS_psi)/Fs ;

        psi_beta_r_e += ((M/tau_r)*ibeta - psi_beta_r_e*(1/tau_r) +
psi_alpha_r_e*omega_MRAS_psi)/Fs;

        flux_error = psi_beta_r_a*psi_alpha_r_e -
psi_alpha_r_a*psi_beta_r_e;

        omega_MRAS_psi = GP_MRAS_psi*(flux_error) + integral_MRAS_psi;

        if(omega_MRAS_psi >= omega_M_nenn)
        {
                omega_MRAS_psi = omega_M_nenn;
```

```c
                integral_MRAS_psi = 0.0;
        }
        else if(omega_MRAS_psi <= 0.0)
        {
                omega_MRAS_psi =  0.0;
                integral_MRAS_psi = 0.0;
        }
        else
        {
                integral_MRAS_psi += GI_MRAS_psi*(flux_error);

                if(integral_MRAS_psi >= omega_M_nenn)
                        integral_MRAS_psi = omega_M_nenn;
                else if(integral_MRAS_psi <= 0.0)
                        integral_MRAS_psi = 0.0;
        }

        omega_MRAS_psi_filter += 0.005*(omega_MRAS_psi -
omega_MRAS_psi_filter);
}

// observer for rotor flux

void rotor_flux_observer(float *psi_r_alpha, float *psi_r_beta,
float ialpha, float ibeta, float omega, float Fs)
{
        *psi_r_alpha += ((M/tau_r)*ialpha - *psi_r_alpha*(1/tau_r) -
*psi_r_beta*omega)/Fs ;

        *psi_r_beta  += ((M/tau_r)*ibeta  - *psi_r_beta *(1/tau_r) +
*psi_r_alpha*omega)/Fs;
}



// flux controller with Anti-Windup

void flux_controller(float target_flux, float flux, float *tar_id)
{
        static float integral_flux = 0.0;

        *tar_id = GP_flux*(target_flux-flux) + integral_flux;


        if (*tar_id > imax)
        {
                *tar_id = imax;
                integral_flux = 0.0;
        }
        else if (*tar_id < i_flux_min)
        {
                *tar_id = i_flux_min;
        }
        else
        {
```

```
              integral_flux += GI_flux*(target_flux - flux);

              if(integral_flux> +3.5)
                    integral_flux= +3.5;
              else if(integral_flux< 0.0)
                    integral_flux= 0.0;
       }
}


// speed controller with Anti-Windup (PI-Controller)

void speed_controller(float target_omega, float omega, float
*tar_iq)
{
       static float integral_omega = 0.0;

       *tar_iq = GP_omega*(target_omega - omega) + integral_omega;

       if (*tar_iq > imax)
       {
              *tar_iq = imax;               // upper limit
              integral_omega = 0.0;
       }
       else if (*tar_iq < 0.0)
       {
              *tar_iq = 0.0;                // lower limit
              integral_omega = 0.0;
       }
       else
       {
              integral_omega +=
GP_omega*GP_omega*GI_omega*(target_omega - omega);

              if(integral_omega> imax)
                    integral_omega= imax;              // upper limit
              if(integral_omega< 0.0)
                    integral_omega= 0.0;               // lower limit
       }
}


// Implementation

void control_system(void)
{
       static int hexcode;
       static float target_psi_d = 0.0;
       static float target_omega_m;
       static float tar_id = 0.0, tar_iq = 0.0;
       static float psi_r_alpha=0.0, psi_r_beta= 0.0;
       static float magnitude_psi_s= 0.0;
       static float angle_theta_k;
       static float counter;
       static float omega_m_filter=0;
       static float phi_k = 0.0;
```

```c
    /* save registers */
    isr_start();

    _get_measurements();

    hexcode = readHex();
    writeHex(hexcode);

    // ======== estimators - controllers - calculations ========

    target_psi_d =          1.1*(float)(hexcode & 0x000F);
    target_omega_m =        200.0*(float)((hexcode & 0x00F0)>>4);

    //speed filter
    omega_m_filter += 0.5*(omega_m - omega_m_filter);

    // 1 estimate flux
    rotor_flux_observer(&psi_r_alpha, &psi_r_beta, ialpha, ibeta,
omega_MRAS_q_filter, Fs);

    // 2 solve angle and magnitude
    karth_polar(&magnitude_psi_s, &angle_theta_k, psi_r_alpha,
psi_r_beta);

    // 3 flux control
    flux_controller(target_psi_d, magnitude_psi_s, &tar_id);


    // 4 speed estimator
    speed_estimator_MRAS_q();

    // 5 speed control
    speed_controller(target_omega_m, omega_MRAS_q_filter,
&tar_iq);

    // field orineted control
    FOC(tar_id, tar_iq, angle_theta_k);


    writeDAC1(magnitude_psi_s,omega_m_filter*0.01);
    writeDAC2(target_omega_m*0.01,iq);

    /* restore registers  */
    isr_end();

    return(IRQ_HANDLED);
}

void estimate_Rs(void)
{

    static int hexcode;
    static long alpha_sample = 0;
    static long beta_sample = 0;
    static int satflag = 0;
    static float tar_id;
```

```c
        static float tar_iq=0;
        static float ulpf1;
        static int counter;
        static float angle = 0.0;
        static float idlpf1,idlpf2;
        static float a;
        static float omega_m_f;

        /* save registers */
        isr_start();

        _get_measurements();

        hexcode = readHex();
        writeHex(hexcode);

         // ======== estimators - controllers - calculations

        tar_id  = 3.43*(float)(hexcode & 0x000F);
        tar_iq  = 0;

        FOC(tar_id, tar_iq, 0.0);

        if (counter < 12205)
                counter++;
        else
        {
                counter = 0;

                printString("R_s = ");
                printFloat(Ud*2/3*Udc/id);
                printString(" Ohm; ");
                printLine(); printLine();

        }

        writeDAC1(tar_id, id);
        writeDAC2(tar_iq, iq);

        /* restore registers  */
        isr_end();

        return(IRQ_HANDLED);

}

void estimate_L_ls(void)
{

        static int hexcode;
        static long alpha_sample = 0;
        static long beta_sample = 0;
        static int satflag = 0;
        static float tar_id;
        static float tar_iq=0;
        static int counter;
```

```c
        static float u, toggle;

        /* save registers */
        isr_start();

        _get_measurements();

        hexcode = readHex();
        writeHex(hexcode);

        // ======== estimators - controllers - calculations

        tar_id   = 3.43*(float)(hexcode & 0x000F);
        tar_iq   = 0;

        FOC(tar_id, tar_iq, 0.0);

        toggle = !toggle;
        if (toggle)
        {
                u = 20.0/(2.0/3.0*Udc);
                Ualpha += u;
        }
        else
        {
                u= -20.0/(2.0/3.0*Udc);
                Ualpha += u;
        }

        writeDAC1(tar_id, id);
        writeDAC2(Ualpha, u);

        // PWM
        SVM(Ualpha, Ubeta, &satflag);

        /* restore registers  */
        isr_end();

        return(IRQ_HANDLED);

}

void flux_psi_r_d(void)
{
        static int hexcode;
        static long alpha_sample = 0;
        static long beta_sample = 0;
        static int satflag = 0;
        static float tar_id;
        static float tar_iq=0;
        static float ulpf1;
        static int counter;
        static float angle = 0.0;
        static float idlpf1;
        static float idlpf2;
        static float a;
```

```
        static float omega_m_f;

        /* save registers */
        isr_start();

        _get_measurements();

        hexcode = readHex();
        writeHex(hexcode);

        // ======== estimators - controllers - calculations

        tar_id  = 3.43*(float)(hexcode & 0x000F);
        tar_iq  = 0.0;

        a += 0.001*(float)((hexcode & 0x0F00)>>8);

        if(a>PI)
                a-=TWOPI;

        FOC(tar_id, tar_iq, a);

        omega_m_f +=  0.001*(omega_m -omega_m_f);

        if (counter < 12205)
                counter++;

        else
        {
                counter = 0;

                printString("psi_r^d = ");
                printFloat(((Uq*2.0/3.0*Udc)-(R_s*iq))/omega_m);
                printString(" Vs; ");
                printLine(); printLine();

        }

        writeDAC1(tar_id, id);
        writeDAC2(iq, a);

        /* restore registers  */
        isr_end();

        return(IRQ_HANDLED);

}

void rotor_time_constant(void)
{

        static int hexcode;
        static long alpha_sample = 0;
        static long beta_sample = 0;
        static int satflag = 0;
        static float tar_id;
```

```c
        static float tar_iq=0;
        static float ulpf1;
        static int counter;
        static float angle = 0.0;
        static float idlpf1;
        static float idlpf2;
        static float a;
        static float omega_m_f;

        /* save registers */
        isr_start();

        _get_measurements();

        hexcode = readHex();
        writeHex(hexcode);

        // ======== estimators - controllers - calculations

        tar_id   = 3.43*(float)(hexcode & 0x000F);
        tar_iq   = 0.0;

        a += 0.005*(float)((hexcode & 0x0F00)>>8);
        if(a>PI)
              a-=TWOPI;

        FOC(tar_id, tar_iq, a);

        omega_m_f +=  0.001*(omega_m -omega_m_f);

        writeDAC1(tar_id, id);
        writeDAC2(omega_m_f*0.01,a );

        /* restore registers  */
        isr_end();

        return(IRQ_HANDLED);

}
```

REFERENCES

1) A. Abbondanti and M.B. Brennen, "Variable Speed Induction Motor Drives use Electronic Slip Calculator based on Motor Voltages and Currents", IEEE Transactions on Industry Applications, Vol.11, No.5, pp.483-488, October 1975.

2) A.M. Trzynadlowski, "Control of Induction Motor", Academic Press, London, 2001.

3) A.M. Trzynadlowski, "The Field Oriented Principle in Control of Induction Motors", Kluwer Academic Publisher, Norwell, MA, 1994.

4) B.K. Bose, "Modern Power Electronics and AC Drives", Prentice Hall Publication, New Delhi, 2008.

5) C. Attainese and A. Damiano, "Induction Motor Drive Parameters Identification", IEEE Transactions on Power Electronics, Vol.13, No.6, pp.1112-1123, November 1998.

6) C. Schauder, "Adaptive speed identification for vector control of induction motors without rotational transducers", IEEE Transactions on Industry Applications, Vol.28, No.5, pp.1054-1061, October 1992.

7) D.J. Atkinson, P.P. Acarnley and J.W. Finch, "Observers for Induction Motor State and Parameter Estimation", IEEE Transactions on Industry Applications, Vol.27, No.6, pp.1119-1127, December 1991.

8) D.W. Novotny and T.A. Lipo, "Vector Control and Dynamics of AC Drives", Oxford University Press, New York, 1997.

9) E.D. Mitronikas and A.N. Safacas, "An Improved Sensor less Vector-Control Method for an Induction Motor Drive", IEEE Transactions on Industrial Electronics, Vol.52, No.6, December 2005.

10) F. Blaschke, "The principle of field orientation as applied to new transvector closed loop control system for rotating field machines", Siemens Review, Vol.39, No.5, pp.217-220, May 1972.

11) F.Z. Peng and T. Fukao, "Robust Speed Identification for Speed Sensor less Vector Control of Induction Motors", IEEE Transactions on Industry Applications, Vol.30, No.5, pp.1234-1239, October 1994.

12) G. Diana and R.G. Harley, "An Aid for Teaching Field Oriented Control Applied to Induction Machines", IEEE Transactions on Power Systems, Vol.4, No.3, pp.1258-1262, April 1989.

13) G. Yang and T. Chin, "Adaptive Speed identification scheme for a vector controlled speed sensor less inverter induction motor drive", IEEE Transactions on Industry Applications, Vol.29, No.4, pp.820-825, May 1993.

14) G.C. Versghese and S.R. Sanders, "Observers for flux estimation in the induction machine", IEEE Transactions on Industrial Electronics, Vol.35, No.1, pp.85-94, October 1998.

15) G.O. Garcia, R.M. Stephan and E.H. Watanabe, "Comparing the indirect field-oriented control with a scalar method", IEEE Transactions on Industrial Electronics, Vol.41, No.2, pp.201-207, April 1994.

16) G.R. Slemon, "Modelling of Induction machines for Electric Drives", IEEE Transaction on Industrial Applications, Vol.25, No.6, pp.1126-1131, October 1989.

17) H. Kubota and K. Matsuse, "Speed Sensorless Field Oriented Control of Induction Motor with Rotor Resistance Adaptation", IEEE Transactions on Industry Applications, Vol.30, No.5, pp.1219-1224, October 1994.

18) H. Tajima and Y. Hori, "Speed Sensorless Field-Orientation Control of the Induction Machine", IEEE Transactions on Industry Applications, Vol.29, No.1, pp.175-180, February 1993.

19) H. Tajima, G. Guidi and H. Umida, "Considerations about problems and solutions of Speed estimation methods and parameter tuning for speed sensor less vector control of induction motor drives", IEEE Transactions on Industrial Applications, Vol.38, No.5, pp.1282-1289, October 2002.

20) H.A. Toliyat, E. Levi and M. Raina, "A Review for RFO induction motor parameter estimation Techniques", IEEE Transactions on Energy Conversion, Vol.18, No.1, pp.271-283, June 2003.

21) I. Boldea and S.A. Nasar, "Vector Control of AC Drives", CRC Press, 1992.

22) I. Landau, "A hyper stability criterion for model reference adaptive control systems," Automatic Control, IEEE Transactions on Industry Applications, Vol.14, No.5, pp.552-555, October 1969.

23) J. Holtz, "Sensorless Control of AC Machines", IEEE Press Book, 1996.

24) J. Lee, T. Takeshita and N. Matsui, "Stator-Flux-Oriented Sensor less Induction Motor Drive for Optimum Low-Speed Performance", IEEE Transactions on Industry Applications, Vol.33, No.5, pp.1170-1176, October 1997.

25) J.W. Finch and D. Giaouris, "Controlled AC electrical drives", IEEE Transactions on Industrial Electronics, Vol.55, No.1, pp.1-11, February 2008.

26) K. Ohyama and G.M. Asher, "Comparative Analysis of Experimental Performance and Stability of Sensorless Induction Motor Drives", IEEE Transactions on Industrial Electronics, Vol.53, No.1, pp.178-184, February 2006.

27) K. Rajashekara, A. Kawamura, and K. Matsuse, "Speed Sensorless Control of Induction Motors", Introductory paper of Sensorless Control of AC Motor Drives - Speed and Position Sensorless Operation - IEEE Press, pp.1-19, 1996.

28) K.B. Nordin and D.W. Novotny, "The influence of motor parameter deviations in feed forward field orientation drive systems", IEEE Transactions on Industry Applications, Vol.21, pp.1009-1015, July 1985.

29) K.D. Hurst, T.G. Hahetler, G. Griva and F. Profumo, "Zero-speed tacho less IM torque control: simply a matter of stator voltage integration", IEEE Transactions on Industry Applications, Vol.34, No.4, pp.790 -795, August 1998.

30) L. Zhen and L. Xu, "Sensor less Field Orientation Control of Induction Machines based on Mutual MRAS Scheme", IEEE Transactions on Industrial Electronics, Vol.45, No.5, pp.824-831, October 1998.

31) L.B. Brahim and A. Kawamura, "A Fully Digitized Field –Oriented Controlled Induction Motor Drive Using Only Current Sensors", IEEE Transactions on Industrial Electronics, Vol.39, No.3, pp.241-249, June 1992.

32) M. Bodson, J. Chiasson and R.T. Novotnak, "Nonlinear Speed Observer for High Performance Induction Motor Control", IEEE Transactions on Industrial Electronics, Vol.42, No.4, pp.337-343, August 1995.

33) M. Cirrincione and M. Pucci, "An MRAS based sensor less high performance induction motor drive with a predictive adaptive model", IEEE Transactions on Industry Applications, Vol.52, No.2, pp.532-551, December 2005.

34) M. Elbuluk, N. Langovsky and D. Kankam, "Design and Implementation of a Closed Loop Observer and Adaptive Controller for Induction Motor Drives", IEEE Transactions on Industry Applications, Vol.34, No.3, pp.435-443, June 1998.

35) M. Liaw, K. Hsiang and J. Lin, "A Discrete Adaptive Field Oriented Induction Motor Drive", IEEE Transactions on Power Electronics, Vol.7, No.2, pp.411-419, April 1992.

36) M. Marchesoni, P. Segarich and E. Soressi, "A simple approach to flux and speed observation in induction motor drives", IEEE Transactions on Industrial Electronics, Vol.44, No.4, pp.528-535, February 1997.

37) M. Marwali, A. Keyhani and W. Tjanaka, "Implementation of Indirect Vector Control on an Integrated Digital Signal Processor based System", IEEE Transactions on Energy Conversion, Vol.20, No.1, October 1998.

38) M.Shin, D. Hyun, S. Cho and S. Choe, "An Improved Stator Flux Estimation for Speed Sensor less Stator Control of Induction Motors", IEEE Transactions on Industry Applications, Vol.15, No.2, pp.312-317, August 1993.

39) P. Vas and J. Li, "Simulation Package for Vector Controlled Induction Motor Drives", Oxford University press, 1993.

40) P. Vas, "Sensor less Vector and Direct Torque Control", Oxford University Press, New York, 1998.

41) P.C. Krause, O. Wasynczuk and S.D. Sudhoff, "Analysis of Electric Machinery and Drive Systems", IEEE Press, 2002.

42) P.L. Jansen and R.D. Lorenz, "Transducer less position and velocity estimation in induction and salient AC machines", IEEE Transactions on Industry Applications, Vol.31, No.1, pp.240-247, April 1995.

43) R. Bojoi, P. Guglielmi and G.M. Pellegrino, "Sensorless direct field-oriented control of three-phase induction motor drives for low cost applications", IEEE Transactions on Industry Applications, Vol.44, No.2, pp.475-481, March 2008.

44) R. Jotten and G. Maeder, "Control Methods for Good Dynamic Performance of Induction Motor Drives Based on Current and Voltage As Measured Quantities", IEEE Transactions on Industry Applications, Vol.19, No.3, pp.356-363, March 1983.

45) R. Krishna and A.S. Bharadwaj, "A Review of Parameter Sensitivity and Adaptation in Indirect Vector Controlled Induction Motor Drive Systems", IEEE Transactions on Power Electronics, Vol.6, No.1, pp.695-703, October 1991.

46) R. Lorenz, "Tuning of the field oriented induction motor controller for high performance applications", IEEE Transactions on Industry Applications, Vol.22, No.1, pp.293-297, August 1986.

47) R.Krishnan and F.C.Doran, "Study of parameter sensitivity in high performance inverter fed induction motor drive systems", IEEE Transactions on Industry Applications, Vol.23, No.1, pp.623-635, December 1987.

48) S. Bowes and J. Li, "New Robust Adaptive Control Algorithm for High Performance AC Drives", IEEE Transactions on Industrial Electronics, Vol.47, No.2, pp.325-336, April 2000.

49) S. Maiti, C. Chakraborty, Y. Hori and M.C. Ta, "Model reference adaptive controller based rotor resistance and speed estimation techniques for vector controlled induction motor drive utilizing reactive power", IEEE Transactions on Industrial Electronics, Vol.55, No.2, pp.594-601, February 2008.

50) T. Ohtani, "Vector Control of Induction Motor without Shaft Encoder", IEEE Transactions on Industry Applications, Vol.28, No.1, pp.157-164, February 1992.

51) U. Baader, M. Depenbrock and G. Gierse, "Direct self-control (DSC) of inverter fed induction machine - A basis for speed control without speed measurement", IEEE Transactions on Industry Applications, Vol.28, No.1, pp.581-588, June 1992.

52) V.R. Jevremovic, V. Vasic, D.P. Marcetic and B. Jefienic, "Speed sensorless control of induction motor based on reactive power with rotor time constant identification", Electric Power Applications, IET, Vol.4, No.6, pp.462-473, July 2010.

53) W. Leonhard, "Control of Electrical Drives", Springer Verlag Berlin, Germany, 1992.

54) W.L. Erdman and R. G. Hoft, "Induction machine field orientation along air gap and stator flux", IEEE Transactions on Energy Conversion, Vol.5, No.1, pp.115-12, March 1990.

55) Y.D. Landau, "Adaptive Control - The Model Reference Approach", Marcel Dekker (CRC Press), New York, 1979.

56) Y.T. Kao and C.H. Liu, "Analysis and design of microprocessor based vector controlled induction motor drives", IEEE Transactions on Industrial Electronics, Vol.39, No.1, February 1992.